Eocene-Oligocene magnetobiochronology of ODP Sites 689 and 690, Maud Rise, Weddell Sea, Antarctica

Fabio Florindo[†]
Istituto Nazionale di Geofisica e Vulcanologia, Via di Vigna Murata, 605, I-00143 Rome, Italy, and *Southampton Oceanography Centre, University of Southampton, Southampton SO14 3ZH, UK*

Andrew P. Roberts
Southampton Oceanography Centre, University of Southampton, Southampton SO14 3ZH, UK

ABSTRACT

Magnetostratigraphic studies of Paleogene sediments piston-cored on Maud Rise, Weddell Sea (ODP Sites 689 and 690), are a cornerstone of Southern Ocean Paleogene and Neogene chronostratigraphy. However, parts of previous magnetostratigraphic interpretations have been called into question, and recent reinvestigation of the upper Paleocene–middle Eocene portion of Site 690 suggested that the records might be contaminated by spurious magnetizations, which raises doubts about the reliability of these important records. We undertook a high-resolution magnetostratigraphic study of Eocene-Oligocene u-channel samples from ODP Holes 689B, 689D, 690B, and 690C in order to address these concerns. A pervasive overprint appears to be present below the middle Eocene, which compromises magnetobiostratigraphic interpretations for the upper Cretaceous and lower Paleogene. Nevertheless, our new results provide a robust record of geomagnetic field behavior from 38.5 to 25 Ma and confirm the reliability of these sediments for calibration of biostratigraphic datum events during a crucial phase of earth history when major Antarctic ice sheets developed. Also, comparison of magnetozone thicknesses in multiple holes at the same site indicates that ~1.2–1.8 m of the stratigraphic record is missing at each core break, which corresponds to time breaks of 120–360 k.y. Lack of a continuous record within a single hole renders useless spectral analyses for investigating long geomagnetic and paleoclimatic time series. This observation reinforces the need for coring of multiple offset holes to obtain continuous paleoceanographic records. Sedimentary hiatuses have been identified only at the deeper of the two investigated sites (Site 690), which could mark a local response to the onset of the Antarctic Circumpolar Current.

Keywords: Eocene, Oligocene, Ocean Drilling Program, 689, 690, Maud Rise, Antarctica, magnetostratigraphy.

INTRODUCTION

Climate evolution during the Cenozoic largely reflects a trend toward lower temperatures and polar cryospheric development, initially in Antarctica and later in the Northern Hemisphere (Zachos et al., 2001). Analysis of the paleoclimatic, paleoceanographic, and cryospheric evolution of Antarctica and the surrounding Southern Ocean is important for understanding global long-term climatic and oceanographic changes. The Antarctic continent has been located at southern polar latitudes since the Early Cretaceous (ca. 120 Ma) and became more isolated from other continents following the progressive fragmentation of Gondwana during the Cretaceous and Cenozoic (Lawver et al., 1992; DiVenere et al., 1994; Besse and Courtillot, 2002; Lawver and Gahagan, 2003). Despite its polar position, Antarctica is thought to have remained mostly ice-free, vegetated, and with mean annual temperatures above freezing until the initial growth of the East Antarctic Ice Sheet near the Eocene-Oligocene boundary (e.g., Barrett, 1996; Flower, 1999).

Factors other than geographic location are clearly responsible for Antarctica's glaciation, and several hypotheses have been suggested to account for the progressive Cenozoic buildup of its ice sheets. A leading hypothesis is that the tectonic opening of seaways permitted development of the Antarctic Circumpolar Current, which progressively thermally isolated Antarctica by decoupling the warmer subtropical gyres from the Antarctic continent (e.g., Kennett et al., 1974, 1975; Kennett, 1977, 1978; Exon et al., 2001). The breakup of Gondwana caused expansion of the Southern Ocean during the Cenozoic through northward movement of Australia and its southern continental extension, the South Tasman Rise, and through opening of Drake Passage between Patagonia and the Antarctic Peninsula (Weissel and Hayes, 1972; Barker and Burrell, 1977; Cande et al., 2000; Exon et al., 2001; Lawver and Gahagan, 2003). Marine magnetic anomalies and fracture zone and transform fault lineations constrain the age of formation of both these seaways to ca. 31–32 Ma (Lawver and Gahagan, 2003). An important alternative hypothesis is that global cooling resulted from decreasing concentrations of atmospheric CO_2 (Pearson and Palmer, 2000), and that tectonic opening of deep-sea gateways was of secondary importance (DeConto and Pollard, 2003). Chronologically precise records are needed from the Southern Ocean to date the effects of tectonic and other changes and to document the sequence of events in order to make inferences about causality of Antarctic ice sheet development.

In this paper, we present a new high-resolution magnetostratigraphy of Paleogene sediments recovered during Ocean Drilling Program (ODP) Leg 113, at Sites 689 and 690. These sites penetrated the sedimentary cover of Maud Rise in the Weddell Sea sector of the Southern Ocean. Parts of previous magnetostratigraphic interpretations (Spiess, 1990), which have been a key component of Southern Ocean chronostratigraphies, have been called into question by biostratigraphers (Berggren et al., 1995). Recent paleomagnetic analyses from the upper Paleocene–middle Eocene portion of the Maud Rise records also suggest that the paleomagnetic data are contaminated by spurious magnetizations, which raises doubts about the reliability of these important chronostratigraphic records (Ali et al., 2000). In order to clarify these concerns

[†]E-mail: florindo@ingv.it.

GSA Bulletin; January/February 2005; v. 117; no. 1/2; p. 46–66; doi: 10.1130/B25541.1; 13 figures; 1 table.

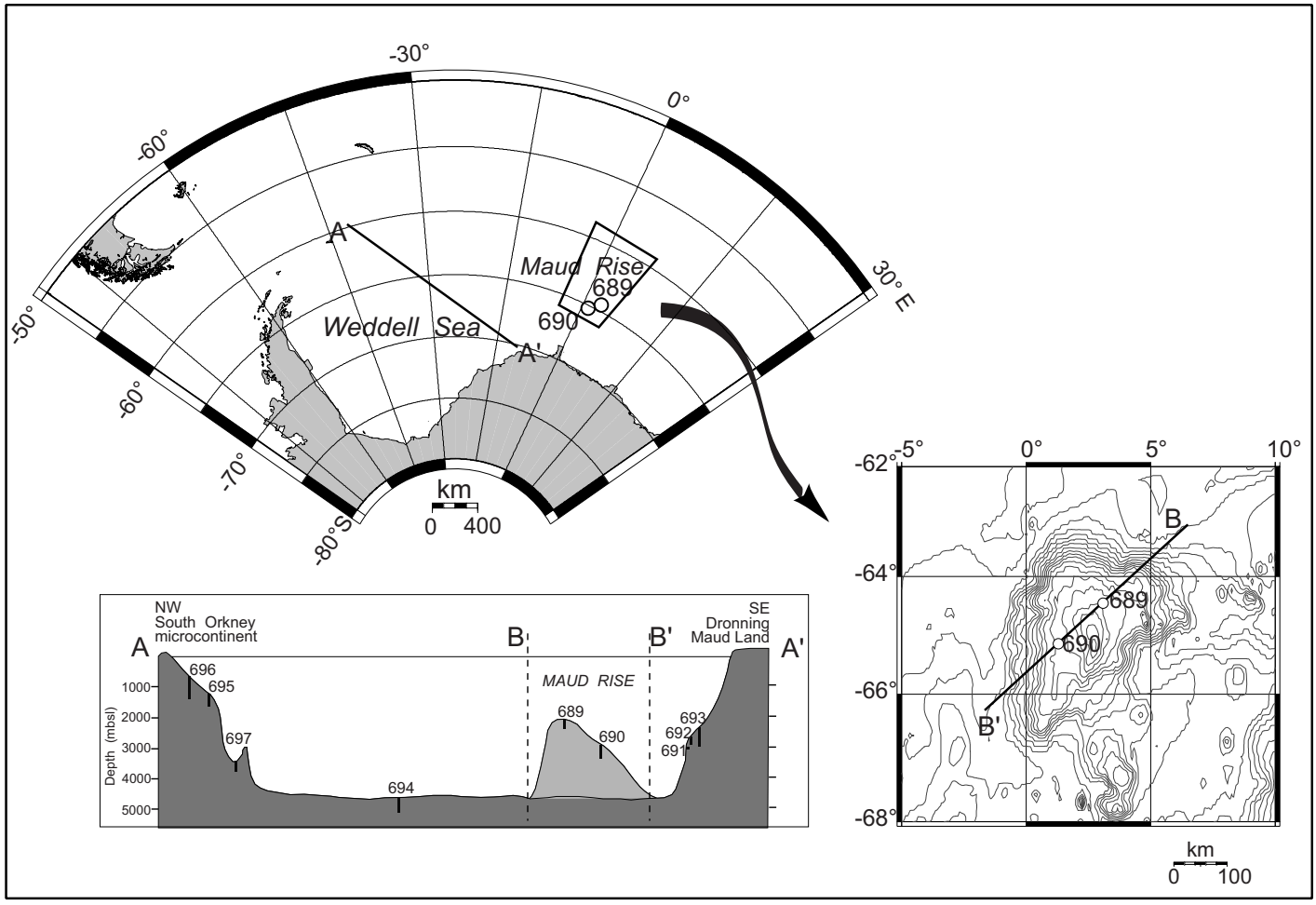

Figure 1. Location map of Maud Rise, with ODP (Ocean Drilling Program) Sites 689 and 690, and schematic northwest-southeast section (A–A′) through the Weddell Sea. A profile across Maud Rise has been projected along the A–A′ section (mbsl—meters below sea level).

and to check the fidelity of the records, a high-resolution paleomagnetic reinvestigation was carried out on these Paleogene sediments.

LOCATION AND SITE DESCRIPTION

During ODP Leg 113, an open-ocean pelagic sedimentary section was cored at two locations on Maud Rise (Sites 689 and 690). Maud Rise (Fig. 1) is presumed to have an oceanic basement that formed via interaction of a spreading ridge with a hot spot (Barker et al., 1988, 1990). Water depths are as shallow as 1800 m, with surrounding deepwater basins extending to depths >5000 m. Maud Rise lies 100 km south of the present-day Polar Front, 100 km north of the Antarctic Divergence and ~700 km from the Antarctic continent (Barker et al., 1988, 1990).

Four holes were cored, using a single advanced piston corer at shallower depths and extended core barrel for the deepest intervals, near the crest of Maud Rise at Site 689 (64°31.01′S; 03°06.00′–03°06.30′E) at a water depth of ~2080 m (Eocene-Oligocene paleodepth 1600 m; Kennett and Barker, 1990). Of these, only Hole 689B provided a nearly continuous sedimentary sequence that is exclusively pelagic and that ranges in age from Late Cretaceous (ca. 75 Ma) to Quaternary (Fig. 2). In general, the Paleogene portion of this record is marked by foraminifer-bearing, calcareous nannofossil ooze and chalk. Biosiliceous facies progressively replaced carbonates from the middle to late Cenozoic, reflecting cooling of the Antarctic water masses.

Three holes were piston-cored at Site 690 (65°09.62′–65°09.63′S; 1°12.29′–1°12.30′E) on the southwestern flank of Maud Rise, 116 km southwest of Site 689, at a water depth of ~2914 m (Eocene-Oligocene paleodepth 2400 m, from Kennett and Barker, 1990). Sites 689 and 690 form part of a depth transect for studies of vertical water-mass stratification around Antarctica during the latest Mesozoic and Cenozoic. The lithologies at Site 690 are similar to those at Site 689. However, the different water depths gave rise to differences in calcite dissolution and/or to winnowing of the sediments. For example, a distinct terrigenous component found at Site 690 is not evident at the shallower Site 689.

PREVIOUS PALEOMAGNETIC INVESTIGATIONS

Cenozoic Magnetostratigraphy of Holes 689B and 690B

A medium-resolution paleomagnetic study of the Maud Rise sites was carried out by Spiess (1990), which provided the first high-quality magnetostratigraphy in the Southern Ocean for a large portion of the Cenozoic. Holes 689B and 690B were investigated over the same age intervals, although the distribution and range of sedimentary hiatuses, mainly identified by diatom biostratigraphy, vary in some parts of the

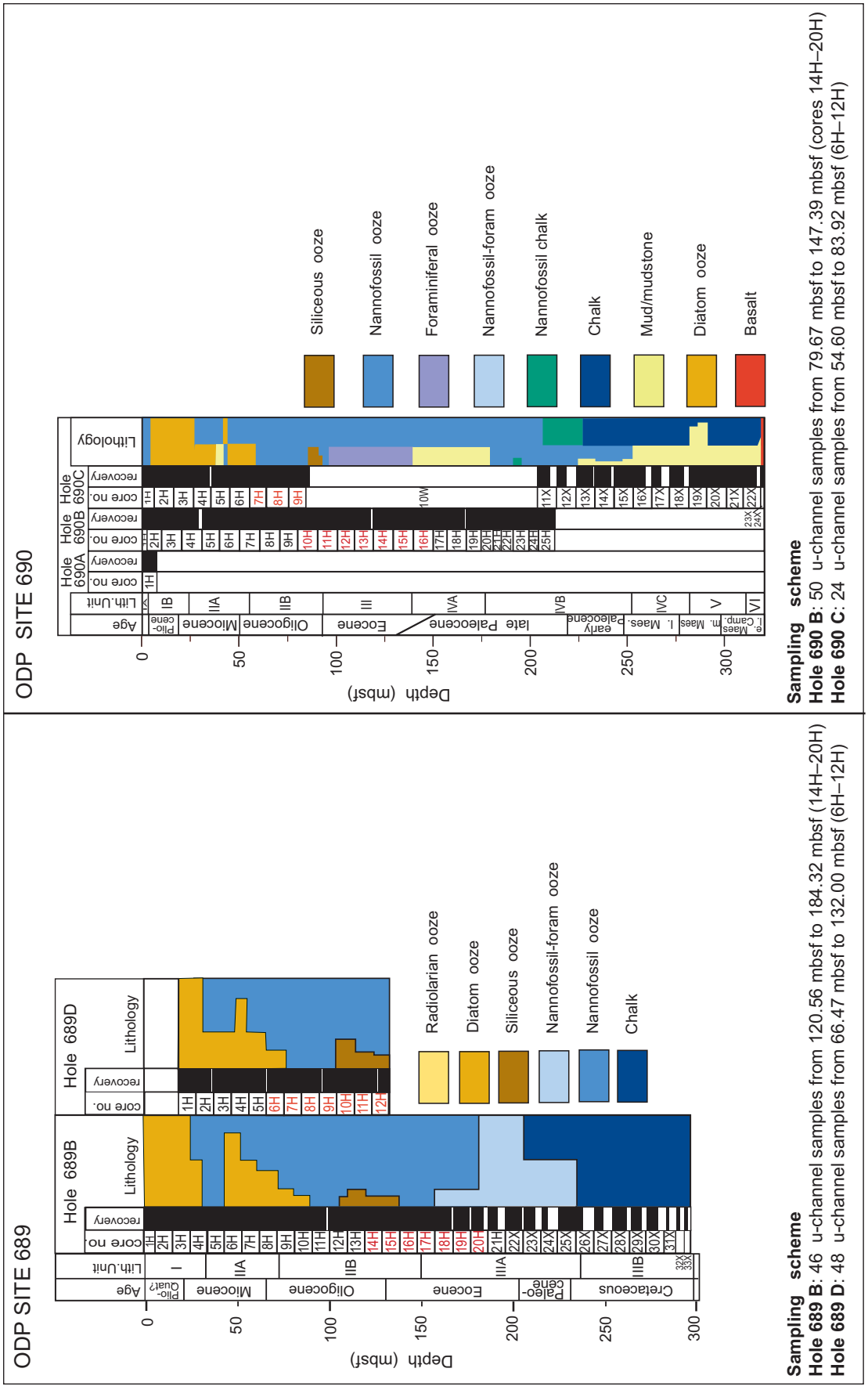

Figure 2. Lithostratigraphic summary logs for ODP Sites 689 and 690 (after Barker et al., 1988). mbsf—meters below seafloor.

records. All of the cores lack azimuthal orientation, but this does not pose a problem for magnetostratigraphic studies since a geocentric axial dipole (GAD) field at the latitude of the drill sites (64–65°S) has a steep inclination (±77°). Paleomagnetic inclinations of the characteristic remanent magnetization (ChRM) are therefore sufficient to uniquely determine polarity.

During ODP Leg 113, the shipboard long-core cryogenic magnetometer system was not correctly functioning, therefore detailed paleomagnetic analyses were carried out after the cruise on discrete samples collected at 25 cm intervals (six samples per 1.5 m core section). Most of the remanence measurements were carried out using a three-axis cryogenic magnetometer (Cryogenic Consultants GM 400) at the University of Bremen. The discrete samples were treated using stepwise alternating field (AF) demagnetization at successive peak fields of 5, 10, 15, 20, 30, 40, and 50 milliTesla (mT), and in a few cases, three additional steps up to 95 mT were added. Generally, secondary components of magnetization were removed at peak fields of 10–20 mT, and in the majority of cases, a stable ChRM component was clearly isolated. Interpretation of the magnetic polarity zonation for both holes was constrained predominantly using diatom and radiolarian datums for the Neogene and Quaternary and using calcareous microfossils for the Miocene and older sequences (Thomas et al., 1990). The geomagnetic polarity time scale (GPTS) of Berggren et al. (1985) was used for the chronostratigraphic interpretation. Some of the magnetic polarity zones were defined on the basis of a single sample, and consequently, resampling with higher resolution was expected in order to confirm some of the interpretations of Spiess (1990).

The reliability of the upper Paleocene–lower Eocene chronostratigraphic interpretations for Hole 690B, which were based on the magnetostratigraphic record, has been questioned by Aubry et al. (1996). These authors pointed out that a ~10 m thick dominantly normal polarity magnetozone, which encompasses the boundary between nannofossil zones NP9 and NP10, has no equivalent in the GPTS (e.g., Berggren et al., 1995). Another mismatch occurs within the apparent record of Chron C25n, which in the published section extends well into NP7, which makes the start of the chron ~1 m.y. older than in the time scale of Berggren et al. (1995).

Reliability of Paleomagnetic Data from Hole 690B

Ali and Hailwood (1998) tried to resolve the possible problems associated with the magnetostratigraphy of the Paleocene-Eocene boundary from Deep Sea Drilling Project (DSDP) Sites 549 and 550 and from ODP Hole 690B. They reported a consistent declination cluster in upper Paleocene–middle Eocene sediments from Hole 690B and in most of the other piston cores from that hole. In order to clarify these concerns, a limited paleomagnetic reinvestigation was carried out based on 98 new paleomagnetic samples from the upper Paleocene to lower–middle Eocene in Hole 690B (Ali et al., 2000) (cores 14H–25H, which span the interval from 125.53 to 213.13 mbsf). Most of the samples have a stable ChRM component perpendicular to the split face of the cores, which provides further evidence for the presence of spurious magnetizations. For azimuthally unoriented cores, randomly oriented core-mean declinations would be expected. In contrast, in many remagnetized ODP cores, clustered declinations are widely observed (e.g., Fuller et al., 1998; Acton et al., 2002b). Moreover, inclination data for some stratigraphic intervals of Hole 690B have values that are noticeably shallower than those expected for a time-averaged GAD field (i.e., 129–133 mbsf and 202–213 mbsf). Ali et al. (2000) interpreted these directions either as a manifestation of an "inward-radial magnetization" (Fuller et al., 1998) or as a "core-split overprint" (Witte and Kent, 1988). Viscous storage overprints, acquired in the repository during several years of storage, have also been reported for similar sediments of similar age (e.g., Touchard et al., 2003). In order to extract a magnetostratigraphy from the upper Paleocene to lower–middle Eocene portion of Hole 690B, Ali et al. (2000) applied a filtering scheme to eliminate overprinted levels from the record. Ali et al. (2000) also concluded that inspection of data from other levels within Hole 690B suggests the same pervasive declination cluster and warn that, before using these magnetostratigraphic data to provide age control, paleomagnetic reinvestigations should be undertaken to establish whether the cores carry secondary overprints that mask the original polarity.

A New High-Resolution Magnetostratigraphy from Eocene-Oligocene Sediments

Maud Rise Sites 689 and 690 still represent key calibration sections for Southern Ocean Eocene-Oligocene biostratigraphic zonations. However, the need to clarify the extent of the spurious magnetizations, and the possibility of obtaining a long, high-quality record of geomagnetic field behavior, prompted this high-resolution magnetostratigraphic reinvestigation. Below, we present results of our new paleomagnetic analyses for the Paleogene portion of the Maud Rise cores, including, where appropriate, correlation of the identified magnetozones to the GPTS. The revised time scale of Cande and Kent (1992, 1995), with biostratigraphic calibrations by Berggren et al. (1995), has been used to interpret the observed polarity zonations. Following major advances in radioisotopic dating, magnetostratigraphy and biostratigraphy, the GPTS has evolved since publication of the previous Cenozoic time scale (Berggren et al., 1985), which was used by Spiess (1990). The identification of new polarity events, based on a reanalysis of marine magnetic anomaly profiles, and assignment of new ages for polarity intervals (Cande and Kent, 1995) required reexamination of all data sets previously used for standardization of the Maud Rise records to the revised time scale.

METHODS

Sampling Procedures

ODP Holes 689B (cores 14H–20H, from 120.56 to 182.82 mbsf), 689D (cores 6H–12H, from 66.47 to 132.00 mbsf), 690B (cores 10H–16H, from 79.67 to 147.36 mbsf), and 690C (cores 7H–9H, from 54.60 to 83.92 mbsf) were sampled, using u-channels, at the ODP East Coast Repository, Lamont-Doherty Earth Observatory, USA. The sampling scheme was designed to provide continuous coverage from the middle Eocene to the late Oligocene, with a record of the Eocene-Oligocene boundary (Fig. 2). A sampling overlap enables continuity of correlation between Holes 689D and 689B and between Holes 690C and 690B.

U-channels are open-sided 2 cm × 2 cm square cross-sectioned liners, up to 1.5 m in length, that are made of transparent, nonmagnetic plastic (Tauxe et al., 1983; Nagy and Valet, 1993; Weeks et al., 1993). After removing the sediment-filled u-channel from the core, an airtight cover was clipped over the u-channel to hold the sediment in place and to prevent it from drying. The u-channel ends were sealed using nonmagnetic laboratory film and tape to minimize moisture loss. The u-channels were taken from the center of the split-core sections, which is the region least affected by coring disturbances and magnetic overprints related to coring with the advanced hydraulic piston corer (Acton et al., 2002a, 2002b). For some intervals, because the sediment was more lithified and/or dried, a clean stainless steel (or ceramic) knife was used to cut the core sections in two parallel lines 2 cm apart. This sampling method produces less disturbance than sampling with conventional cubic samples since the affected surface area/volume ratio is much lower (Weeks et al., 1993). A "way-up" arrow was marked on the u-channel prior to its removal from the core.

Laboratory Procedures and Analysis

U-channel samples were analyzed within the magnetically shielded paleomagnetic laboratory at the Istituto Nazionale di Geofisica e Vulcanologia, Rome, using a narrow-access pass-through cryogenic magnetometer (2-G Enterprises model 750R) with in-line, AF demagnetization capability. The natural remanent magnetization (NRM) was measured at 1 cm stratigraphic intervals, although smoothing occurs due to the Gaussian shape of the response curve of the magnetometer pickup coils (the half-power width suggests smoothing across 4.8 cm for the radial x and y directions and 5.9 cm for the axial z direction) (Weeks et al., 1993). Data from the upper and lower 6 cm of each u-channel were not used because these data are affected by end effects due to the width of the magnetometer response function.

The NRM was subjected to stepwise AF demagnetization at applied fields of 10, 20, 30, 40, 50, 60, 80, and 100 mT. ChRM inclinations were used to determine polarity, where negative inclinations indicate normal polarity intervals and positive inclinations indicate reversed polarity intervals (in the Southern Hemisphere). The sediments are stably magnetized and data from the 20–30 mT steps could be used to estimate the ChRM direction, but where necessary, ChRM components were determined from multiple demagnetization steps using principal component analysis (Kirschvink, 1980). Demagnetization results were examined using orthogonal vector component diagrams, stereographic projections and intensity decay curves.

A range of rock magnetic measurements was made to determine the magnetic mineralogy of the studied sediments. These results will be reported in detail in a future paper. Nevertheless, relatively low coercivities imply that magnetite (and/or low-Ti titanomagnetite) is the primary remanence carrier. Hysteresis parameters are consistent with the presence of pseudo–single-domain magnetite (Day et al., 1977) in a narrow grain size range. No evidence of "wasp-waisted" hysteresis characteristics was detected, which is consistent with a uniform mineralogy and a narrow range of grain sizes (Roberts et al., 1995; Tauxe et al., 1996).

RESULTS

Hole 690C

Significant down-core fluctuations in the NRM intensity are not related to lithological variations (Figs. 2 and 3). NRM values range between 0.23 and 19.36 mA/m, with a mean of 5.66 mA/m. Generally stable paleomagnetic behavior was observed in stepwise AF demagnetization data from Hole 690C. Typical demagnetization behavior is shown in Figure 4A. Most of the analyzed samples have a low-coercivity, subvertical, normal polarity overprint, which is interpreted to represent an isothermal remanent magnetization (IRM) that was imparted during coring or core retrieval (e.g., Fuller et al., 1998; Acton et al., 2002b). This magnetic overprint was successfully removed with peak AFs of 10 mT, and a stable ChRM is evident for a large proportion of the analyzed sediments. This steep magnetic overprint is evident in histograms of the NRM directions (Fig. 5), where there is a broad distribution of inclinations between −90° and −55°. The ChRM inclinations have a much cleaner, clear bimodal distribution, which demonstrates the presence of two stable polarity states. In conjunction with evidence from vector component diagrams (Fig. 4A), this indicates that our demagnetization procedures have successfully removed the secondary remanences. The ChRM declinations undergo a 180° shift at each polarity transition, as would be expected, as well as abrupt shifts at core breaks where different cores would be expected to have different relative orientations (Fig. 3). In addition, other declination shifts are evident within polarity zones, which probably result from twisting and mechanical rotation of the sediment during coring. As a result, the inclination data provide the clearest basis for interpretation of the magnetostratigraphy.

The magnetic polarity data for the studied interval (~54–84 mbsf) are shown in Figure 3. There is a clear square-wave inclination signal with seven distinct magnetozones, four of normal polarity (N1 to N4) and three of reversed polarity (R1 to R3). We identify several short polarity intervals in addition to those identified by Spiess (1990), which we attribute to the higher resolution provided by u-channel samples relative to the previous analysis of discrete samples. The u-channel data also indicate that some of the short polarity intervals identified by Spiess (1990) are probably artifacts of deformation related to coring or sampling, or misorientation of a sample, or measurement error. It is worth noting that intermediate paleomagnetic inclinations were not observed at the boundary between cores 8H and 9H in Hole 690C, which may indicate a time (or coring) gap between magnetozones N3 and R3. Comparing the magnetozone thicknesses from this record (Hole 690C) with those of corresponding magnetozones from Hole 690B (Spiess, 1990), it is possible to estimate the amount of sediment missing at the respective core breaks. Comparison of results from the two studies indicates that ~1.2–1.8 m of sediment is missing at core breaks.

Hole 690B

NRM values for Hole 690B (Fig. 6) are close to those recorded in Hole 690C (Fig. 3). Stable paleomagnetic behavior was generally observed in stepwise AF demagnetization data from cores 10H–14H of Hole 690B (Fig. 4B). Again, most of the analyzed samples have a low-coercivity, normal polarity, coring-induced magnetic overprint. The dominance of demagnetization behavior like that shown in Figure 4B means that it is straightforward to construct a magnetic polarity zonation for the studied interval of Hole 690B, where we observe 14 distinct magnetozones, seven of normal polarity (N1 to N7) and seven of reversed polarity (R1 to R7). In three cases, the inclination record contains short intervals with anomalous inclinations associated with core breaks. These anomalous directions might be related to deformation resulting from coring (i.e., between 79.73 and 80.4 mbsf, between 89.2 and 89.5 mbsf, and between 118.6 and 119.0 mbsf) (Barker et al., 1988). In two additional cases, corresponding to breaks between cores 11H and 12H and between cores 12H and 13H (Fig. 6), the boundary between magnetozones is indicated by sharp shifts in inclination, which suggests that a significant amount of time might be missing at these core breaks (Fig. 6).

The steep paleomagnetic inclinations provide a clear indication of the polarity, and the clear square-wave paleomagnetic signal, with bimodal inclinations that coincide with the expected value for a GAD field at the site latitude (Fig. 5), suggests that the magnetic polarity signal is robust for Hole 690B. In addition to careful inspection of vector component diagrams (Fig. 4B), this evidence indicates that any secondary magnetic overprints have been adequately removed by AF demagnetization. Below core 14H (128.10 mbsf), the magnetizations are weaker and are much less stable than for the upper sediments (Figs. 4C and 4D). We therefore do not present results below this depth.

Hole 689D

The sediments from Hole 689D generally give stable univectorial paleomagnetic directions after removal of a low-coercivity, normal polarity, coring-induced overprint with peak AF of 10 mT (Fig. 4E). Variable magnetic overprints are evident in histograms of the NRM inclinations (Fig. 5). Nevertheless, after AF demagnetization, the ChRM declinations shift by 180° at each polarity transition, and the ChRM inclinations have a clear bimodal distribution that demonstrates the presence of two stable polarity states (Fig. 7). The normal and

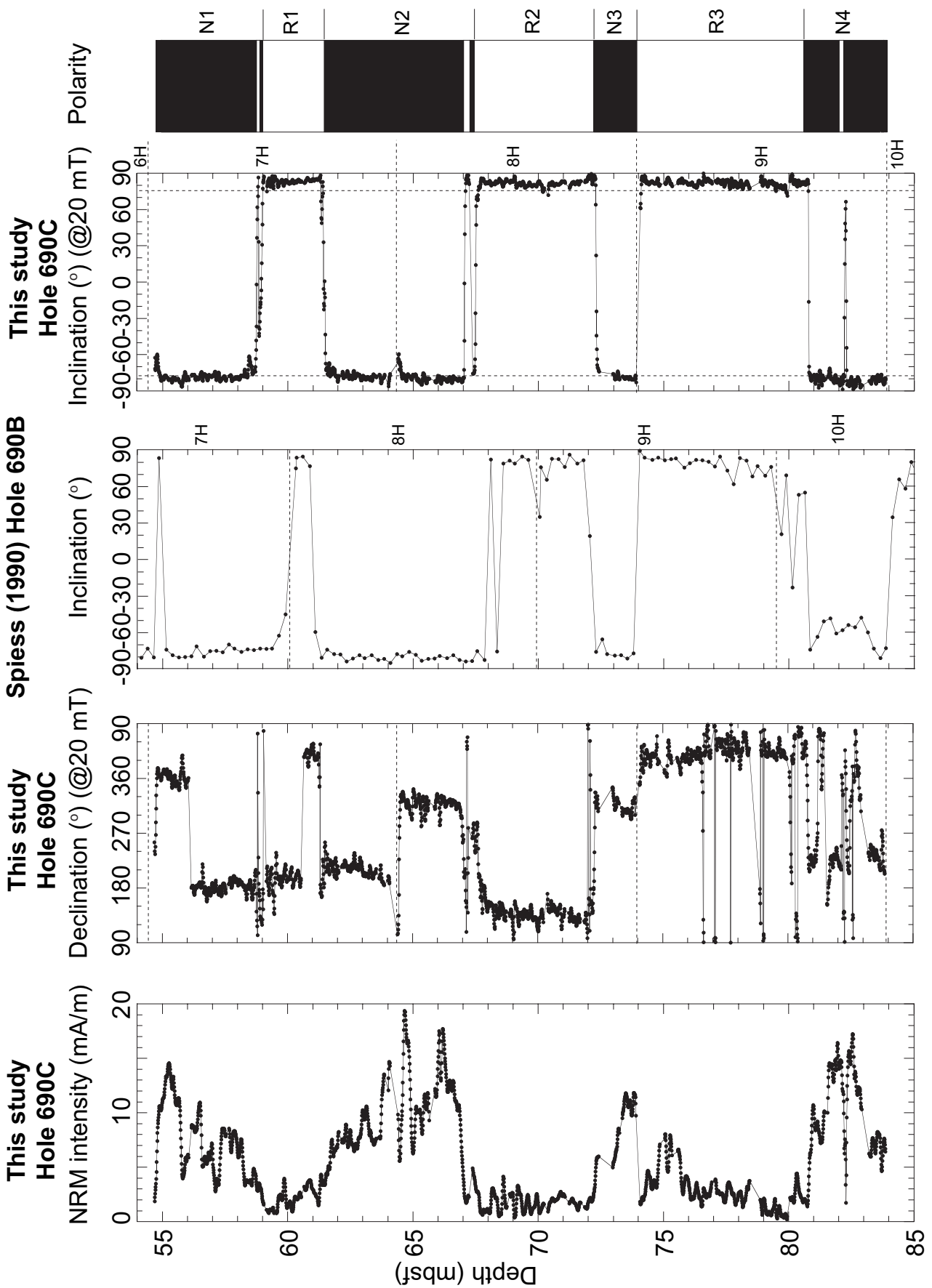

Figure 3. Down-core variations in the NRM intensity for Hole 690C (this study), declination for Hole 690C (this study), inclination for Hole 690B (Spiess, 1990), and inclination for Hole 690C (this study). The magnetic polarity zonation is shown on the log to the right. Black (white) represents normal (reversed) polarity intervals. NRM—natural remanent magnetization. mbsf—meters below seafloor.

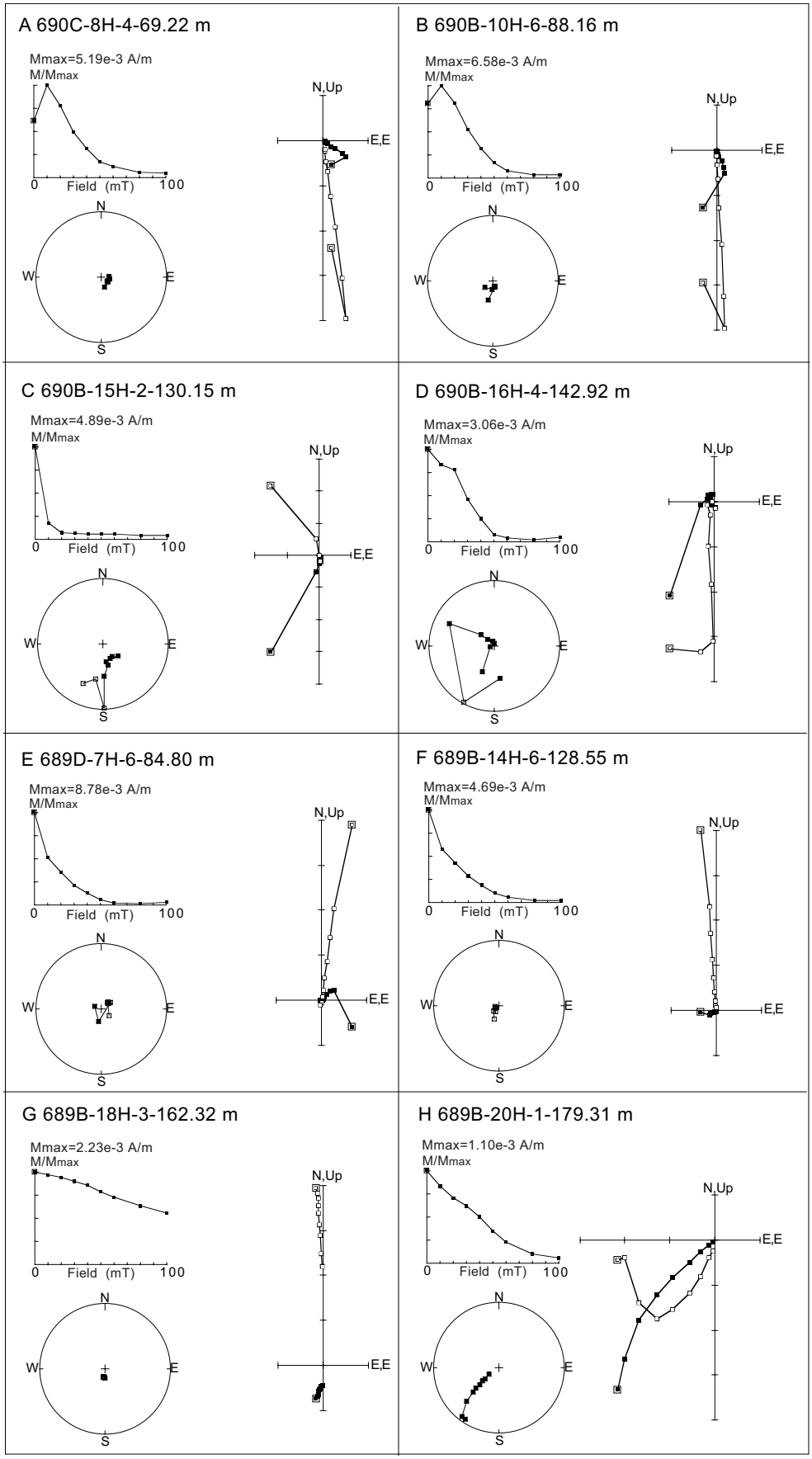

Figure 4. AF (alternating field) demagnetization behavior for eight representative stratigraphic levels from Holes 690C, 690B, 689D, and 689B. For the vector component diagrams, open (closed) symbols represent projections onto the vertical (horizontal) plane. The stereoplots are equal-area stereographic projections, where solid (open) symbols represent lower (upper) hemisphere projections. The cores were not azimuthally oriented; declinations are reported in the laboratory coordinate system with respect to the split face of the drill core. Mmax refers to the maximum magnetization measured during AF demagnetization of the NRM intensity.

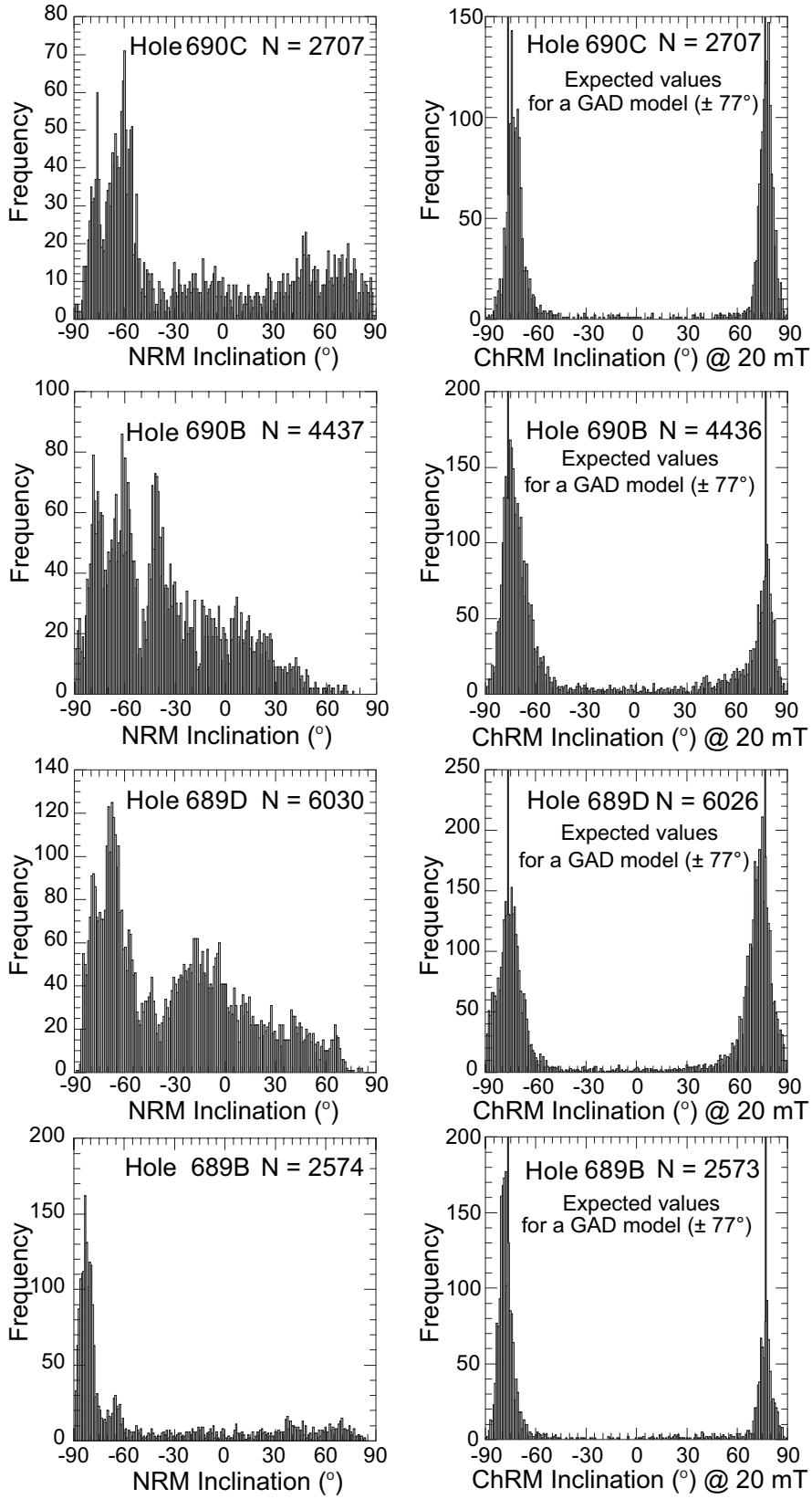

Figure 5. Histogram of NRM and ChRM inclinations, respectively, for Holes 690C, 690B, 689D, and 689B. The expected inclinations for a GAD field at the site latitude are also shown. The statistical mode for normal and reversed polarity data for these holes is coincident with the expected GAD values. NRM—natural remanent magnetization. ChRM—characteristic remanent magnetization. GAD—geocentric axial dipole.

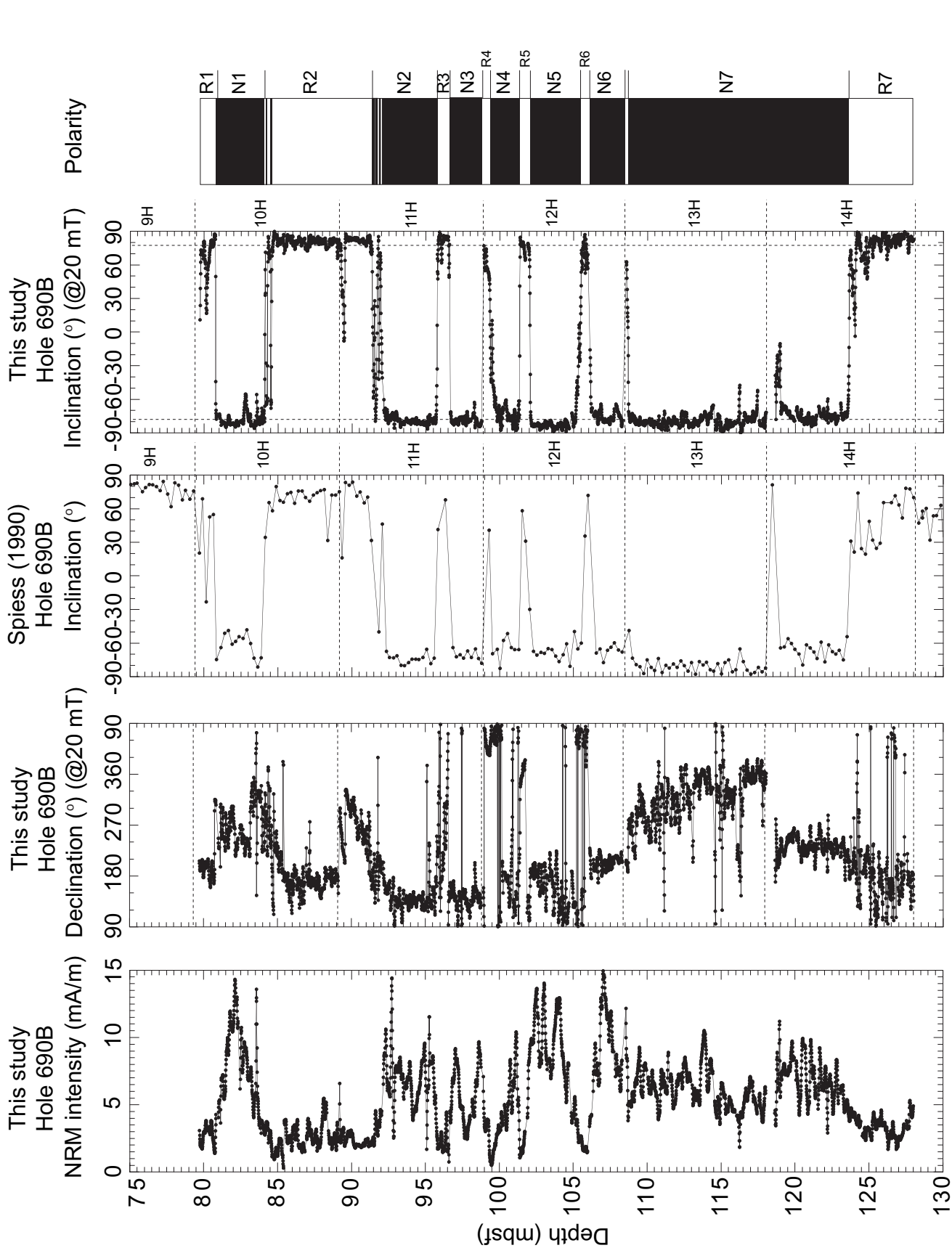

Figure 6. Down-core variations in the NRM intensity for Hole 690B (this study), declination for Hole 690B (this study), inclination for Hole 690B (Spiess, 1990), and inclination for Hole 690B (this study). The magnetic polarity zonation is shown on the log to the right. Black (white) represents normal (reversed) polarity intervals. NRM—natural remanent magnetization. mbsf—meters below seafloor.

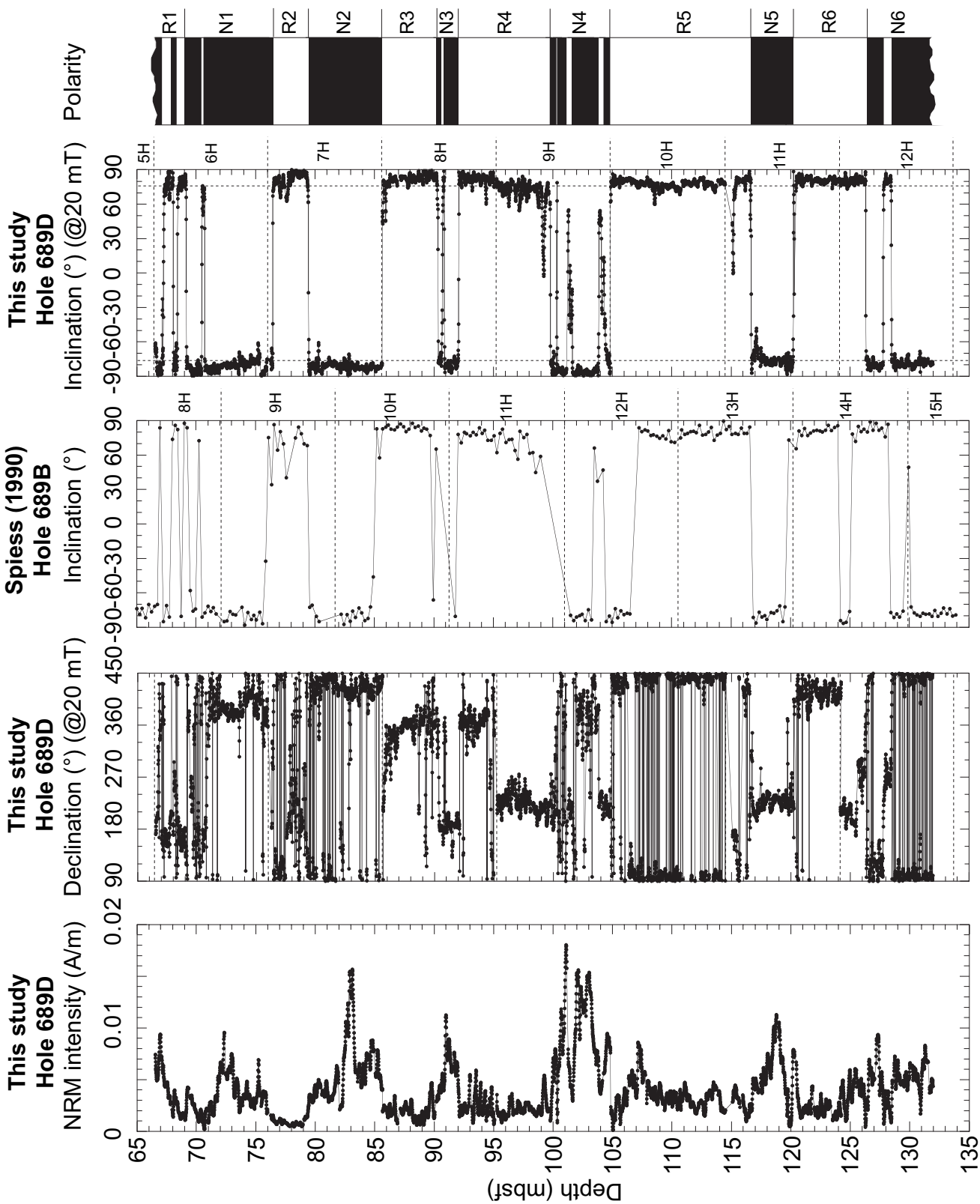

Figure 7. Down-core variations in the NRM intensity for Hole 689D (this study), declination for Hole 689D (this study), inclination for Hole 689B (Spiess, 1990), and inclination for Hole 689D (this study). The magnetic polarity zonation is shown on the log to the right. Black (white) represents normal (reversed) polarity intervals. NRM—natural remanent magnetization. mbsf—meters below seafloor.

reversed polarity ChRM inclinations are indistinguishable from expected GAD field values for the site latitude (Fig. 5). In conjunction with evidence from vector component diagrams, this indicates that demagnetization has successfully removed any secondary magnetization components. The ChRM inclinations clearly define a series of magnetozones, labeled from R1 to N6 (Fig. 7). The polarity intervals are bounded by polarity transitions only a few centimeters in thickness. In two cases, corresponding to core breaks, the boundary between the magnetozones is indicated by sharp shifts in inclination (i.e., 85.6 and 104.8 mbsf). This indicates that an unspecified amount of section is missing at these core breaks.

As is the case for Hole 690C, by comparing the magnetozone thicknesses from Hole 689D in the interval between 99.0 and 105.0 mbsf with the corresponding magnetozones from Hole 689B (Spiess, 1990), it appears that ~1.7 m of section is missing at the core break between cores 9H and 10H in Hole 689D (Fig. 7). In addition, the short reversed polarity interval observed at ~101.3 mbsf in Hole 689D is not recorded in Hole 689B because of the core break at 101.0 mbsf.

Hole 689B

Stable paleomagnetic behavior was also generally observed in stepwise demagnetization data from cores 14H to 16H of Hole 689B (120.62–148.85 mbsf) (Fig. 8). Typical demagnetization behavior is shown in Figure 4F. A ChRM is isolated after removal of a low-coercivity, nearly vertical, coring-induced magnetic overprint at 10–20 mT. This dominantly vertical magnetic overprint is evident in histograms of the NRM inclinations, in which there is a statistical mode at around −85° (Fig. 5). The ChRM inclination values from the stable polarity intervals are grouped in two antipodal clusters that are compatible with the expected GAD inclination values at the site latitude (Fig. 5).

Significant down-core fluctuations are evident in the NRM intensity that are not related to lithological variations in Hole 689B (Fig. 8). A major down-core decrease in NRM intensity is recorded at 144.30 mbsf. The ChRM inclinations clearly define a series of magnetozones (R1 to N4). Comparison of this record with the Hole 689B magnetostratigraphy of Spiess (1990) suggests that the two short reversed polarity intervals based on single discrete samples (at 129.94 mbsf and 139.5 mbsf) are related to disturbances at core breaks.

By analogy to core 690B-14H, starting from core 689B-17H the paleomagnetic signal becomes less stable, with a progressive loss of the square-wave inclination signal. Shallow paleomagnetic inclinations and, at some levels, clustering of declinations and higher coercivities appear in this lower portion of Hole 689B (Figs. 4G and 4H). This observation is consistent with those of Ali et al. (2000) for the upper Paleocene to lower-middle Eocene section of Hole 690B, and care must be taken when interpreting the paleomagnetic signal from such intervals.

DISCUSSION

Correlation with the GPTS

Based on the clear square-wave magnetostratigraphic signal observed for the paleomagnetic declination and inclination data from Maud Rise, we interpreted the intervals of core discussed above to contain a robust magnetostratigraphy (Figs. 3, 6, 7, 8). This means that a large portion of the studied record can be used for developing a high-quality magnetobiostratigraphic record. However, the lower parts of the studied intervals appear to be affected by the remagnetization suggested by Ali et al. (2000). We therefore refrain from interpreting these lower intervals.

In the following discussion, we provide an interpretation of the magnetic polarity pattern of the stably magnetized portions of Holes 689B, 689D, 690B, and 690C, using the established Southern Ocean calcareous nannofossil zonation (Wei and Thierstein, 1991; Wei and Wise, 1992; Wei, 1992). The GPTS used in these studies was that of Berggren et al. (1985). The numerical ages given in this paper have therefore been adjusted to ensure consistency with the newer GPTS of Berggren et al. (1995) and Cande and Kent (1995). Where necessary, we also considered new quantitative analyses of calcareous nannofossil assemblages (Persico and Villa, 2002, 2004). These new analyses have the advantage of utilizing several prominent high-latitude species, while retaining datums for temperate marker species that penetrate the high southern latitudes. The other microfossil groups play only a limited role in constraining Paleogene events at Sites 689 and 690. Our magnetostratigraphic interpretation for Holes 689B, 689D, 690B, and 690C are presented in Figures 9, 10, 11, and 12 along with biostratigraphic datums and the stratigraphic uncertainties associated with each datum (see Table 1 for details).

Hole 689D

The nannofossil bioevents recorded in the studied portion of Hole 689B (Table 1) (Wei and Wise, 1992; Wei, 1992) fall on or near the correlation line between our magnetic polarity zonation and the GPTS (Berggren et al., 1995) (Fig. 9). Of these events, the last occurrence (LO) of *Reticulofenestra bisecta* and the LO of *Chiasmolithus altus* (N1 and N2, respectively, which both occur at an average depth of 66.55 mbsf) do not fall on the magnetostratigraphic correlation line, which might reflect either the low sampling resolution for the biostratigraphic analysis (one sample from every 1.5 m core section or two samples per core section in some intervals), or reworking. This latter hypothesis is supported by new quantitative analyses (at a 10 cm sampling interval) of calcareous nannofossil assemblages (Persico and Villa, 2002, 2004). These authors identified datum N2 at 72.40 mbsf and (very) rare occurrences of *Chiasmolithus altus* and *Chiasmolithus* spp. above this level are considered to have been reworked.

Correlation of the paleomagnetic polarity pattern with the GPTS provides a direct age interpretation between the upper Eocene and the upper Oligocene (from Chron C16n.2n to C7n.2n). The only mismatch with the GPTS is the absence of the normal polarity Chron C15n (34.66–39.94 Ma). Comparison of our results from Hole 689D and those of Spiess (1990) from Hole 689B demonstrate that C15n is present in Hole 689B, but that it is missing in the core break between cores 11H and 12H in Hole 689D (Fig. 7).

Our magnetostratigraphic interpretation is supported by the calcareous nannofossil biostratigraphy and by identification of the rapid >1‰ step in $\delta^{18}O$ (Oi-1 event) at ~120 mbsf in Hole 689B (Stott and Kennett, 1990; Thomas et al., 1990; Diester-Haass and Zahn, 1996) and by a major shift in clay mineral assemblages (Ehrmann and Mackensen, 1992). The Oi-1 event occurred at the base of Chron C13n. On the basis of the above correlation to the GPTS, the average sedimentation rate for the studied interval of Hole 689D was ~0.6 cm/k.y.

Hole 689B

In order to extend our analysis at Site 689 further into the Eocene, it was necessary to switch from Hole 689D to Hole 689B (Figs. 2 and 10). Our magnetostratigraphic interpretation for the middle-upper Eocene (from Chron C18n.1n to C13r) of Hole 689B is broadly consistent with the available biostratigraphic constraints (Fig. 10; Table 1). In addition, the horizon at 128.70 mbsf, which is interpreted to represent the clinopyroxene-bearing spherule-strewn field and the North American tektite-strewn field combined, provides an $^{40}Ar/^{39}Ar$ date of 35.5 Ma for this level (Glass et al., 1986; Vonhof et al., 2000) that supports our interpretation.

The uppermost ~12 m of the studied portion of Hole 689B overlaps the lower part of Hole 689D. In Hole 689D, Chron C15n is missing at the core break between cores 11H and 12H at

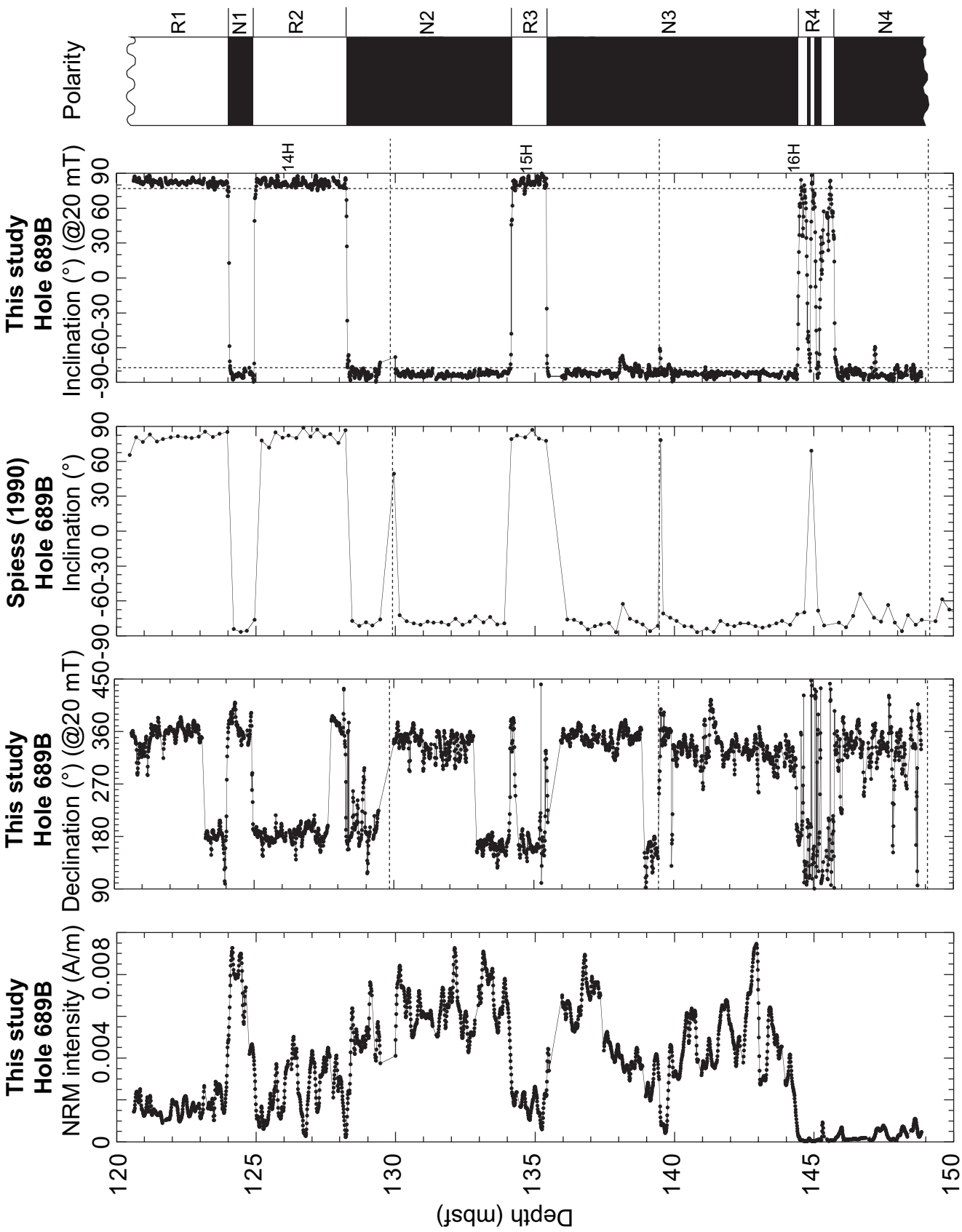

Figure 8. Down-core variations in the NRM intensity for Hole 689B (this study), declination for Hole 689B (this study), inclination for Hole 689B (Spiess, 1990), and inclination for Hole 689B (this study). The magnetic polarity zonation is shown on the log to the right. Black (white) represents normal (reversed) polarity intervals. NRM—natural remanent magnetization. mbsf—meters below seafloor.

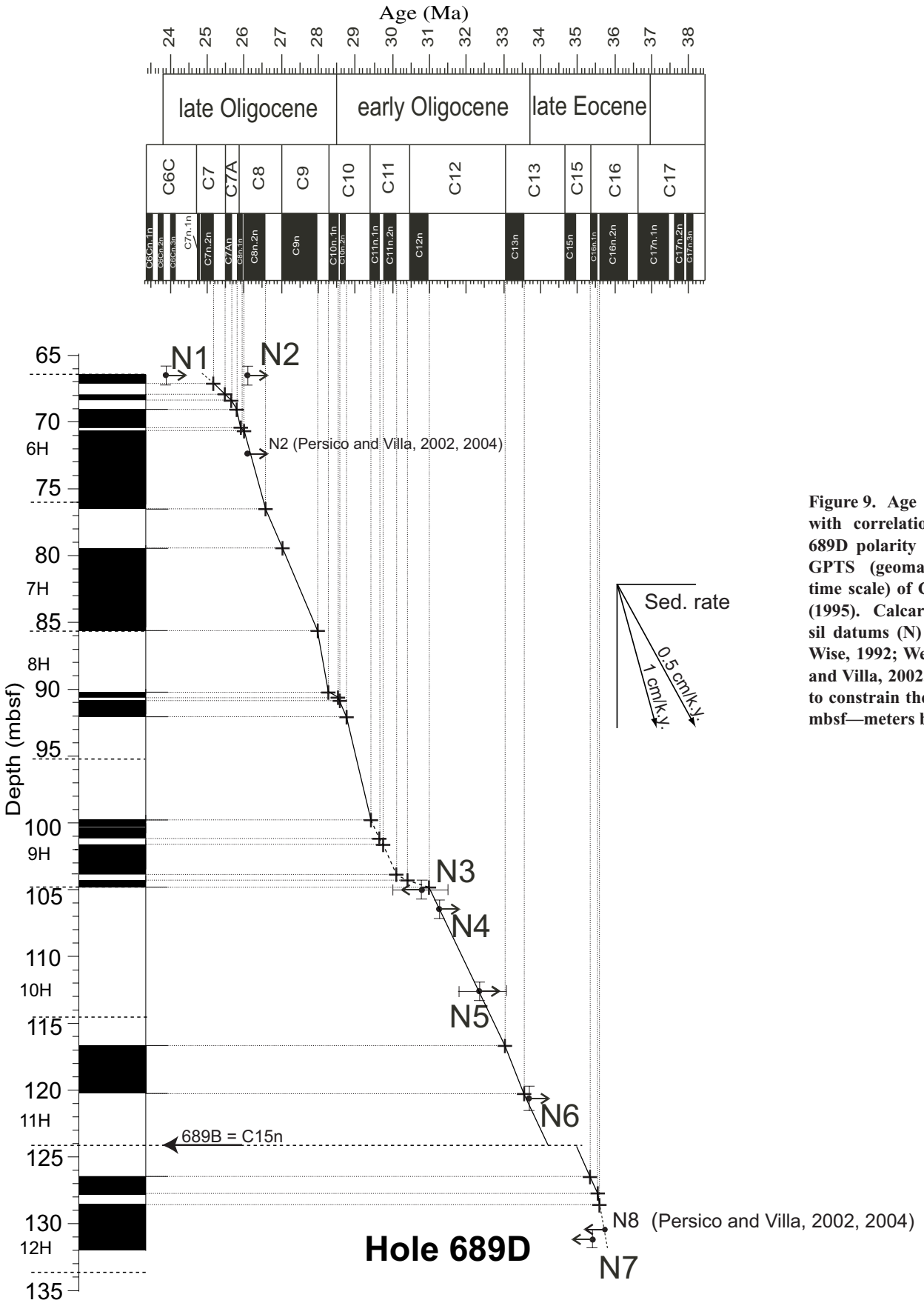

Figure 9. Age vs. depth plot with correlation of the Hole 689D polarity zonation to the GPTS (geomagnetic polarity time scale) of Cande and Kent (1995). Calcareous nannofossil datums (N) (from Wei and Wise, 1992; Wei, 1992; Persico and Villa, 2002, 2004) are used to constrain the interpretation. mbsf—meters below seafloor.

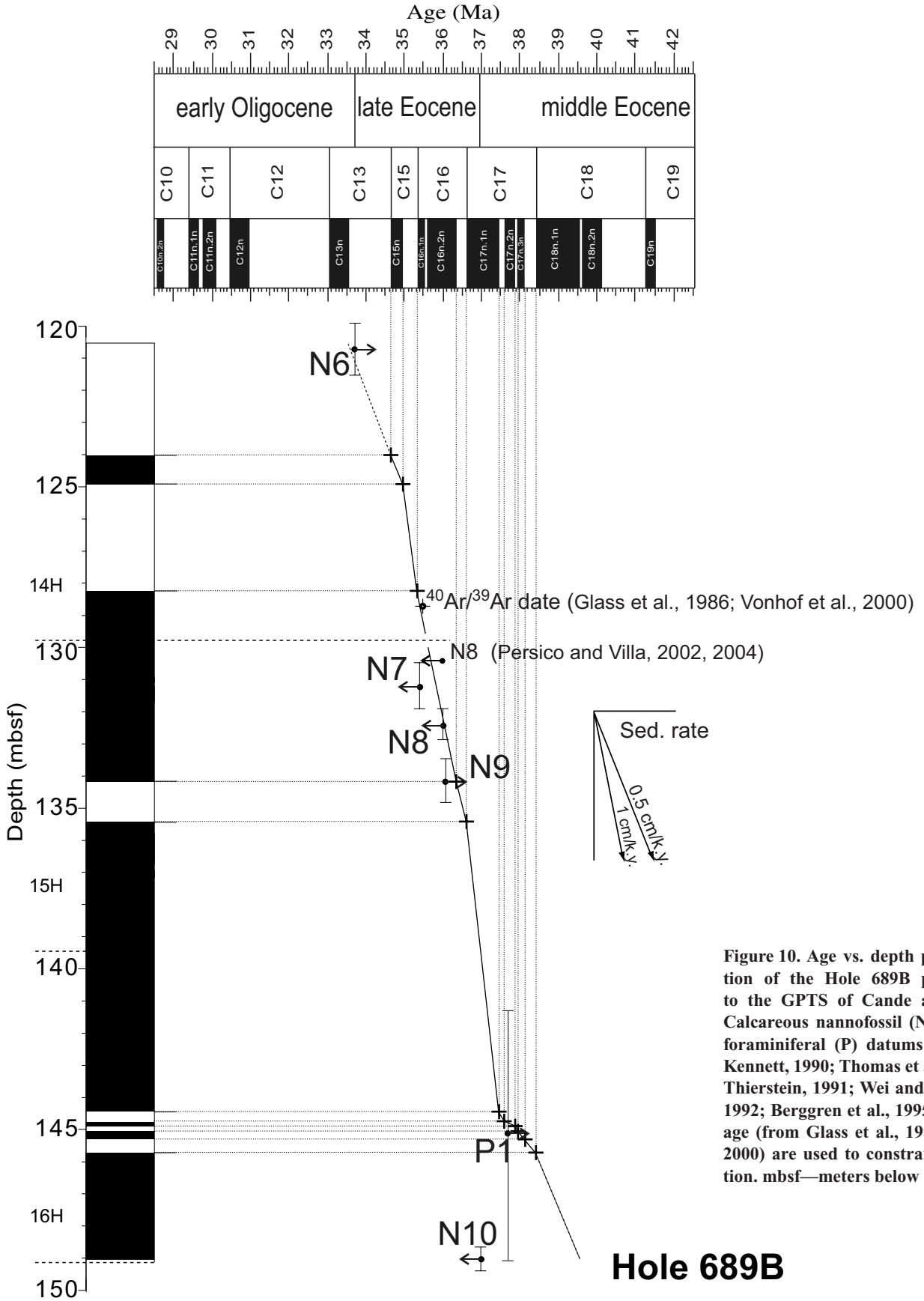

Figure 10. Age vs. depth plot with correlation of the Hole 689B polarity zonation to the GPTS of Cande and Kent (1995). Calcareous nannofossil (N) and planktonic foraminiferal (P) datums (from Stott and Kennett, 1990; Thomas et al., 1990; Wei and Thierstein, 1991; Wei and Wise, 1992; Wei, 1992; Berggren et al., 1995) and a $^{40}Ar/^{39}Ar$ age (from Glass et al., 1986; Vonhof et al., 2000) are used to constrain the interpretation. mbsf—meters below seafloor.

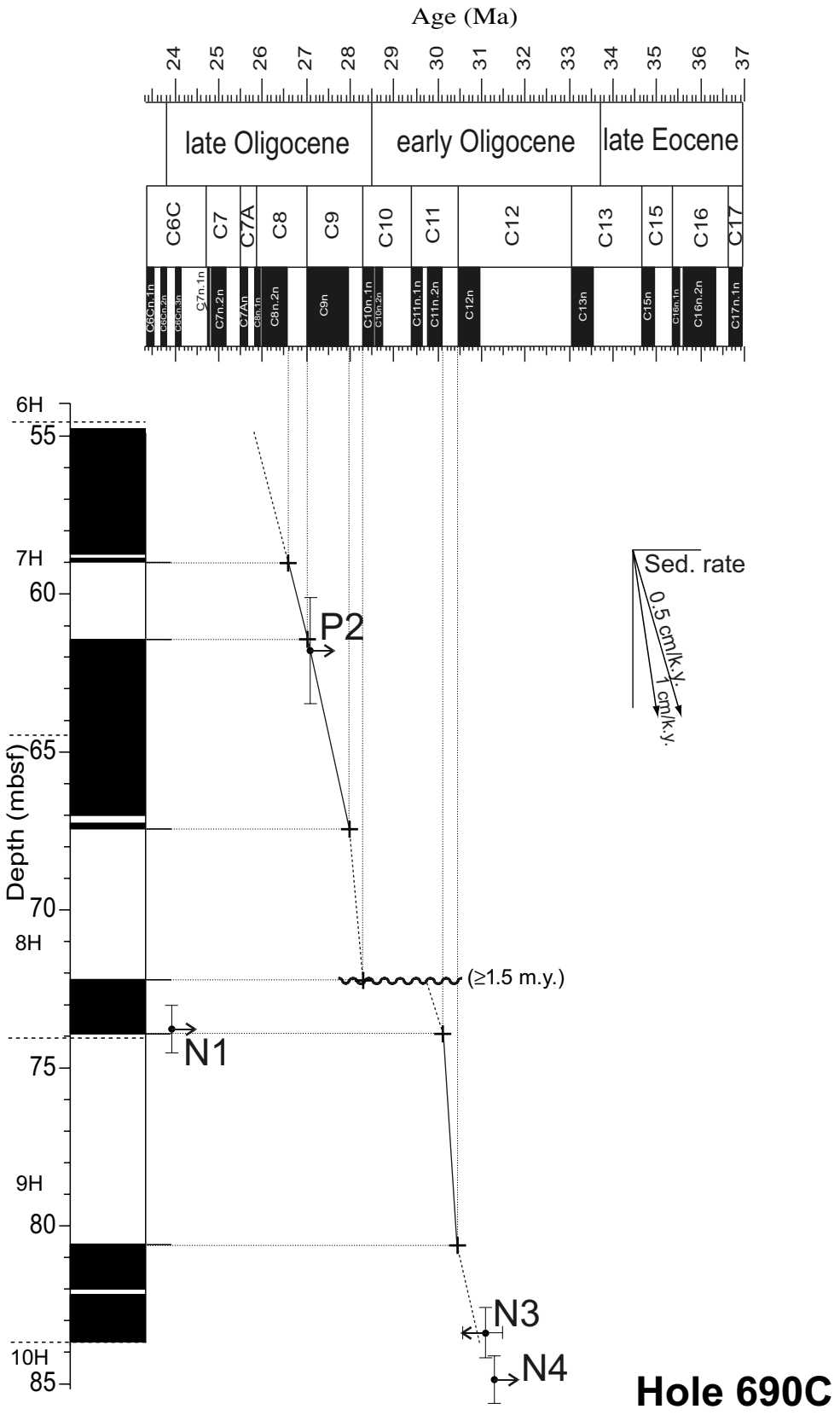

Figure 11. Age vs. depth plot with correlation of the Hole 690C polarity zonation to the GPTS of Cande and Kent (1995). Calcareous nannofossil datums (N) and planktonic foraminiferal (P) datums (from Stott and Kennett, 1990; Thomas et al., 1990; Wei and Thierstein, 1991; Wei and Wise, 1992; Wei, 1992; Berggren et al., 1995; Persico and Villa, 2002, 2004) are used to constrain the interpretation. mbsf—meters below seafloor.

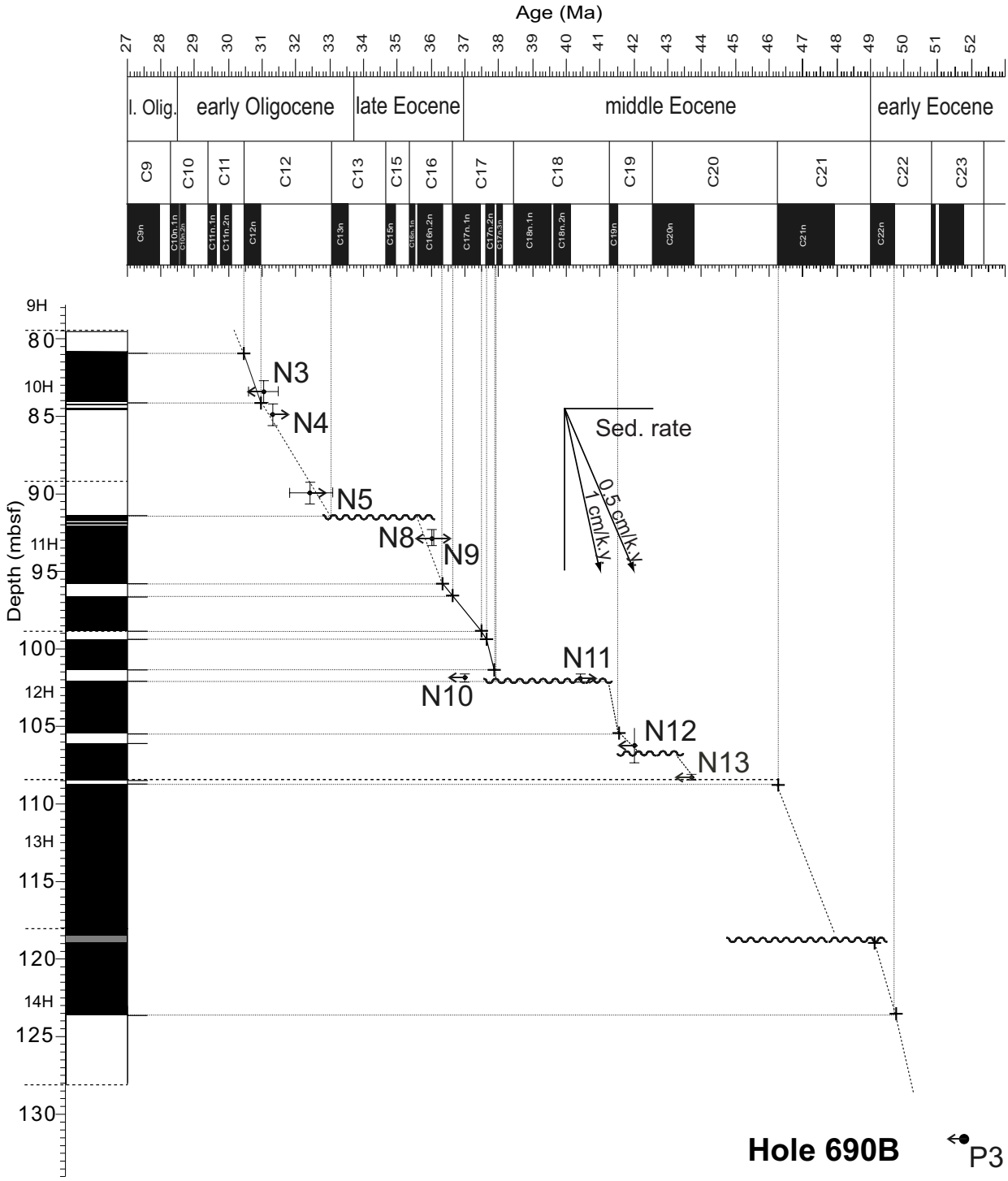

Figure 12. Age vs. depth plot with correlation of the Hole 690B polarity zonation to the GPTS of Cande and Kent (1995). Calcareous nannofossil (N) and planktonic foraminiferal (P) datums (from Stott and Kennett, 1990; Thomas et al., 1990; Wei and Thierstein, 1991; Wei and Wise, 1992; Wei, 1992; Berggren et al., 1995) are used to constrain the interpretation. mbsf—meters below seafloor.

TABLE 1. DEPTH RANGES OF CALCAREOUS NANNOFOSSIL DATUMS

Designation	Biostratigraphic datum	Sample present	Depth (mbsf)	Average depth (mbsf)	Age (Ma)
Hole 689B					
N1	LO *Reticulofenestra bisecta*	8H-3, 30/ 8H-4, 30	65.80–67.30	66.55	23.9
N2	LO *Chiasmolithus altus*	8H-3, 30/ 8H-4, 30	65.80–67.30	66.55	26.1
N3	FO *Cyclicargolithus abisectus*	12H-3, 29/12H-5, 29	104.29–105.70	105.04	31.3
N4	LO *Reticulofenestra umbilicus*	12H-4, 29/12H-5, 29	105.79–107.20	106.54	31.3
N5	LO *Isthmolithus recurvus*	13H-1, 130/13H-2, 130	111.90–113.40	112.65	31.8–33.1
N6	LO *Reticulofenestra oamaruensis*	13H-7, 28/14H-1, 130	119.88–121.50	120.69	33.7
N7	FO *Reticulofenestra oamaruensis*	15H-1, 28/15H-2, 28	130.40–131.90	131.25	35.4
N8	FO *Isthmolithus recurvus*	15H-2, 30/15H-2, 131	131.90–132.90	132.40	36.0
N9	LO *Reticulofenestra reticulata*	15H-3, 31/15H-4, 31	133.40–134.90	134.20	36.1
N10	FO *Chiasmolithus oamaruensis*	16H-7, 29/17H-1, 29	148.69–149.39	149.04	37.0
N11	LO *Chiasmolithus solitus*	17H-3, 29/17H-4, 29	152.39–153.89	153.14	40.4
N12	FO *Reticulofenestra reticulata*	18H-2, 29/18H-3, 29	160.59–162.09	161.39	42.0
N13	FO *Reticulofenestra umbilicus*	18H-3, 29/18H-4, 29	162.09–163.59	162.84	43.7
Hole 690B					
N1	LO *Reticulofenestra bisecta*	9H-3, 28/9H-4, 28	73.08–74.58	73.83	23.9
N2	LO *Chiasmolithus altus*	7H-1, 130/7H-2, 28	51.20–52.18	51.69	26.1
N3	FO *Cyclicargolithus abisectus*	10H-3, 26/10H-4, 26	82.66–84.16	83.41	31.3
N4	LO *Reticulofenestra umbilicus*	10H4, 26/10H-5, 26	84.16–85.66	84.89	31.3
N5	LO *Isthmolithus recurvus*	11H-1, 29/11H-1, 130	89.39–90.40	89.90	31.8–33.1
N8	FO *Isthmolithus recurvus*	11H-3, 29/11H-3, 130	92.39–93.40	92.90	36.0
N9	LO *Reticulofenestra reticulata*	11H-3, 29/11H-3, 130	92.39–93.40	92.90	36.1
N10	FO *Chiasmolithus oamaruensis*	12H-2, 130/12H-3, 29	101.60–102.20	101.90	37.0
N11	LO *Chiasmolithus solitus*	12H-2, 130/12H-3, 29	101.60–102.20	101.90	40.4
N12	FO *Reticulofenestra reticulata*	12H-5, 29/12H-6, 29	105.09–107.40	106.25	42.0
N13	FO *Reticulofenestra umbilicus*	12H-7, 29/12H, CC	108.07–108.50	108.29	43.7

Note: From Wei (1992), Wei and Wise (1992), modified. All nannofossil ages are calibrated to the Berggren et al. (1995) time scale. Biostratigraphic datums are abbreviated as follows: LO—last occurrence datum, FO—first occurrence datum. mbsf—meters below seafloor.

~124.0 mbsf (Fig. 9), but it is recovered in Hole 689B (Fig. 10). In the same way, in Hole 689B, Chron C16n.1r (35.53–35.69 Ma) is inferred to be missing at the break between cores 14H and 15H (Fig. 10), whereas it is recorded at the bottom of Hole 689D (Fig. 9).

In the basal part of Hole 689B, the first occurrence (FO) of *Chiasmolithus oamaruensis* (N10), lies far from the correlation line, in a normal polarity interval that we correlate to Chron C18n.1n. This datum is reported as falling in Chron C17n.1n at DSDP Site 523 (Poore et al., 1983; Berggren et al., 1995) and at DSDP Site 516 (Wei and Wise, 1989; Berggren et al., 1995), with an age assignment of 37.0 Ma in the time scale of Berggren et al. (1995). This inconsistency could be due to environmental factors, to diachroneity of the species between low and midlatitudes, to a poorly calibrated datum, or to poor sampling resolution (one sample per core section).

Below ~135 mbsf, our correlation to the GPTS is also supported by the LO of the planktonic foraminifer *Subbotina linaperta* (P1 in Fig. 10) at 141.26–149.09 mbsf, which has an age assignment of 37.7 Ma (Stott and Kennett, 1990; Thomas et al., 1990; Berggren et al., 1995), although its range is poorly constrained in Hole 689B. The average sedimentation rate for the studied interval of Hole 689B was ~0.5–1.0 cm/k.y.

Hole 690C

Correlation of our magnetostratigraphy for Hole 690C to the GPTS is mainly constrained by nannofossil datums documented in Hole 690B (Fig. 11; Table 1) (Wei and Wise, 1992). However, between the top of the studied portion of Hole 690C and ~72 mbsf, the record does not contain nannofossil events, and interpretation of the polarity zonation was constrained by the LO of the planktonic foraminifer *Globigerina labiacrassata* (P2 in Fig. 11). This event, which is recorded between 60.10 and 63.48 mbsf, has an age assignment of 27.1 Ma (Stott and Kennett, 1990; Thomas et al., 1990; Berggren et al., 1995) and permits correlation of the thick normal polarity interval between 61.4 and 67.5 mbsf with Chron C9n, which is the longest normal polarity interval in the Oligocene.

In the lower part of the studied record in Hole 690C, the FO of *Cyclicargolithus abisectus* (N3) and the LO of *Reticulofenestra umbilicus* (N4) suggest that the normal polarity interval at the base of the studied interval correlates with Chron C12n (30.48–30.94 Ma). It is worth noting that the LO of *Reticulofenestra bisecta* (N1) is recorded at a mean depth of 73.83 mbsf, which disagrees with our magnetostratigraphic interpretation. New quantitative analyses by Persico and Villa (2002, 2004) demonstrate the rarity of this taxon in Hole 690C, which prevents any meaningful biostratigraphic use of this datum in Hole 690C. Based on biostratigraphic datum P2, we correlate the interval between ~55 and 72.2 mbsf to Chrons C8n.2n through to C9r. A hiatus (≥1.5 m.y. in duration) seems to be present at ~72.2 mbsf. The interval below the hiatus is correlated to the base of C11n.2n, and then to Chron C11r and to the top of Chron C12n. Minimum sedimentation rates above and below the hiatus were ~0.8 and 1 cm/k.y., respectively.

Hole 690B

Magnetostratigraphic interpretation of the early Eocene–early Oligocene portion of Hole 690B is hampered by the presence of a series of sedimentary hiatuses (Fig. 12). We correlate the interval from ~79 mbsf (at the break between cores 9H and 10H) and ~92 mbsf to the base of Chron C11r and to Chrons C12n and C12r, respectively. The FO of *Cyclicargolithus abisectus* (N3) at 83.41 mbsf, and the LO of

Reticulofenestra umbilicus (N4) and *Isthmolithus recurvus* (N5) at 84.89 and 89.90 mbsf, respectively, support our magnetostratigraphic interpretation. Below this interval, the absence of the FO and the LO of *Reticulofenestra oamaruensis* (N6 and N7), and the concomitant presence at 92.90 mbsf of the FO of *Isthmolithus recurvus* (N8) and the LO of *Reticulofenestra reticulata* (N9), require a hiatus of ~2.5 m.y. in duration at ~92 mbsf. This unconformity is visually recognizable in core 690B-11H-3, 73–90 cm (at ~92.8 mbsf). There is considerable reworking up to 40 cm above this unconformity (see Fig. 7 in the Site 690 chapter of Barker et al., 1988). The Eocene-Oligocene boundary, which occurs just below the base of Chron C13n, should lie within the hiatus at ~92.8 mbsf. We correlate the six magnetozones below this unconformity to the base of Chron C16n.2n, and then to Chrons C16r, C17n.1n, C17n.1r, C17n.2n and C17n.2r, respectively. It is worth noting that at the break between cores 11H and 12H, the boundary between the magnetozones is indicated by a sharp shift in inclination, which suggests that an undetermined amount of time is missing (Figs. 6 and 12).

Two other hiatuses have been suggested at ~102 mbsf to explain the juxtaposition of the FO of *Chiasmolithus oamaruensis* (N10) and the LO of *Chiasmolitus solitus* (N11), and at 106.80 mbsf (core 690B-12H-6, 40–55 cm) (see Fig. 8 in Site 690 chapter, Barker et al., 1988). It is difficult to interpret the magnetic polarity pattern in the immediate vicinity of these unconformities. However, based on the FO of *Reticulofenestra reticulata* (N12), the polarity zones between these two unconformities (102.0 and 106.8 mbsf) correlate reasonably well with Chrons C19n and C19r. Another sharp shift in inclination was recorded at the break between cores 12H and 13H, at 108.50 mbsf (Fig. 6), which suggests that the top of the thin reversed polarity interval below this level is truncated. Datum N13 (FO of *Reticulofenestra umbilicus*), which occurs at a mean depth of 108.29 mbsf, suggests that the normal polarity interval between 106.0 and 108.5 mbsf is likely to represent part of Chron C20n. Below N13, no further calcareous nannofossil events constrain the correlation of the paleomagnetic polarity zonation to the GPTS. However, the occurrence of the planktonic foraminifer *Acarinina primitiva* (P3 in Fig. 12), identified at a mean depth of 133.35 mbsf (Stott and Kennett, 1990; Berggren et al., 1995), provides a lower boundary for the age of the investigated interval (top of Chron C23r). The thick normal polarity interval between 108.65 and 123.65 mbsf might therefore represent the juxtaposition of Chron s C21n and C22n. In this case, the reversed polarity interval C21r would be missing in the break between cores 13H and 14H at ~118.70 mbsf. Based on the P3 constraint, the reversed polarity interval at the bottom of the studied portion of Hole 690B might then correlate with the top of Chron C22r.

Erosion Events

Deep-sea hiatuses are generally interpreted as erosional features resulting from strong bottom currents. The sedimentary record at Maud Rise would be expected to contain evidence of erosive events associated with fluctuations of circumpolar deep water as it moved eastward around Antarctica. Sedimentary hiatuses have been identified only at the deepest of the two investigated sites (Site 690; Fig. 13), which suggests a link with strong bottom water flow that caused erosion or nondeposition. Available evidence suggests the presence of a major unconformity at 72.2 mbsf in Hole 690C (which removed Chrons C10n.1n to C11n.2n [Fig. 13]; ca. 28.5–30 Ma), which is coeval with an unconformity documented in ODP Holes 744A and 748B, at water depths of 2308 and 1291 m, respectively, on the southern Kerguelen Plateau (Roberts et al., 2003). These hiatuses are coeval with the opening of Drake Passage to deep water circulation at ca. 31 ± 2 Ma (Lawver and Gahagan, 2003), which provides a strong link between the progressive tectonic opening of Drake Passage and development of the Antarctic Circumpolar Current. This major change in oceanic circulation also appears to have affected intermediate waters because a coeval (30–31 Ma) decrease in sedimentation rates, probably related to increased current winnowing, is observed at the shallower Site 689 on Maud Rise (Fig. 9). Regional synchroneity of these erosive events at Maud Rise and Kerguelen Plateau is likely to reflect wide-scale intensification of bottom current circulation associated with development of the Antarctic Circumpolar Current. At this stage, it is less straightforward to explain the origin of other hiatuses identified in middle-late Eocene sediments at Maud Rise, but they are certainly connected to the evolution of this portion of the Southern Ocean.

CONCLUSIONS

We have conducted a high-resolution magnetostratigraphic study of Eocene-Oligocene u-channel samples from Holes 689B, 689D, 690B, and 690C, drilled during ODP Leg 113, which represent key calibration points for Southern Ocean Paleogene and Neogene biostratigraphic zonations (Fig. 13). Stable paleomagnetic behavior was observed in stepwise AF demagnetization data from these holes, and a pervasive overprint, similar to that previously observed by Ali et al. (2000) and by Ali and Hailwood (1998) in the upper Paleocene–middle Eocene portion of the records, appears to be confined to sediments of middle Eocene and older age. At these levels, we observed shallow paleomagnetic inclinations, clustering of declinations, and, at some levels, high coercivities. Interpretation of the magnetic polarity zonation of the stably magnetized portions of these holes was constrained using the established Southern Ocean calcareous nannofossil zonation (Wei and Wise, 1992; Wei, 1992) and, where necessary, new quantitative analyses of calcareous nannofossil assemblages (Persico and Villa, 2002, 2004). The new results highlight a superb record of geomagnetic field behavior for ~13 million years (from 38.5 to 25 Ma) (Fig. 13).

Comparing the magnetozone thicknesses from our record with those of corresponding magnetozones from parallel holes (Spiess, 1990), we estimate that ~1.2–1.8 m of the stratigraphic record is missing at each core break for the Paleogene Maud Rise sequences, which represents an average time break of 120–360 k.y. This observation has important implications because lack of continuous sediment recovery renders useless spectral analyses of temporally long geomagnetic and paleoclimatic data sets from such records (e.g., Tauxe and Hartl, 1997; Constable et al., 1998; Robert et al., 2002) and reinforces the importance of constructing a composite stratigraphic record using multiple holes at the same site (cf. Hagelberg et al., 1995).

Finally, sedimentary hiatuses have been identified only at the deeper of the two investigated sites (Site 690; Fig. 13), which suggests a link with strong bottom water flow that caused erosion or nondeposition. Of these, a major erosive event is recorded in the late–early Oligocene, which is coeval with an unconformity documented at ODP Holes 744A and 748B on the southern Kerguelen Plateau (Roberts et al., 2003) and with the opening of Drake Passage to deep water circulation at ca. 31 ± 2 Ma (Lawver and Gahagan, 2003). This erosion event could therefore mark a local response to the onset of the Antarctic Circumpolar Current. Other hiatuses are present in the Maud Rise Paleogene record, but their link with major fluctuations of the Antarctic Circumpolar Current is less clear.

ACKNOWLEDGMENTS

We thank the Ocean Drilling Program (ODP) curatorial advisory board for granting permission to work on this valuable archive core material and to ODP personnel at the East Coast Repository at Lamont-Doherty Earth Observatory (LDEO) and Leonardo Sagnotti and Richard Weaver for assistance with

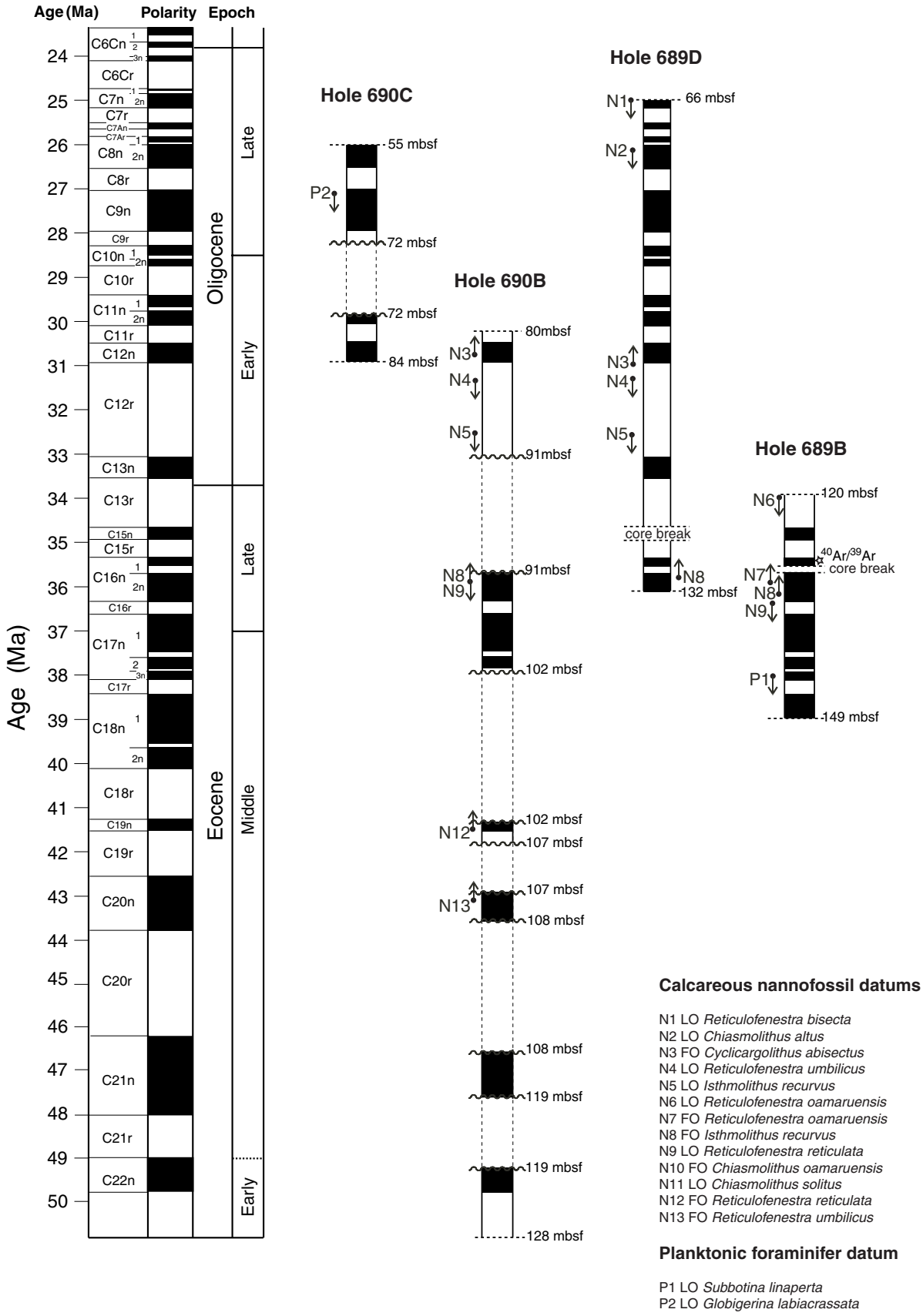

Figure 13. Chronostratigraphic summary of the studied Eocene and Oligocene sediments from Maud Rise. The calcareous nannofossil datums (N) and planktonic foraminiferal (P) datums are the same as in Figures 9, 10, 11, and 12 (see text). mbsf—meters below seafloor.

sampling. Davide Persico and Giuliana Villa kindly gave access to unpublished calcareous nannofossil data. Steven Bohaty, Eelco Rohling, Gary Acton, Jason Ali, and Ken Kodama are thanked for comments that improved aspects of this work. The ODP is sponsored by the U.S. National Science Foundation (NSF) and participating countries (including the UK) under management of Joint Oceanographic Institutions (JOI), Inc. We gratefully acknowledge funding from the Italian Programma Nazionale di Ricerche in Antartide (PNRA) and the National Environmental Research Council (NERC).

REFERENCES CITED

Acton, G.D., Guyodo, Y., and Brachfeld, S.A., 2002a, Magnetostratigraphy of sediment drifts on the continental rise of West Antarctica (ODP Leg 178, Sites 1095, 1096, and 1101), *in* Barker, P.F., et al., eds., Proceedings of the Ocean Drilling Program: Scientific Results, v. 178, p. 1–61, http://www-odp.tamu.edu/publications/178_SR/VOLUME/CHAPTERS/SR178_37.PDF.

Acton, G.D., Okada, M., Clement, B.M., Lund, S.P., and Williams, T., 2002b, Paleomagnetic overprints in ocean sediment cores and their relationship to shear deformation caused by piston coring: Journal of Geophysical Research, v. 107, 2067, doi: 10.1029/2001JB000518.

Ali, J.R., and Hailwood, E.A., 1998, Resolving possible problems associated with the magnetostratigraphy of the Paleocene/Eocene boundary in Holes 549, 550 (Goban Spur) and 690B (Maud Rise): Strata, v. 9, p. 16–20.

Ali, J.R., Kent, D.V., and Hailwood, E.A., 2000, Magnetostratigraphic reinvestigation of the Palaeocene/Eocene boundary interval in Hole 690B, Maud Rise, Antarctica: Geophysical Journal International, v. 141, p. 639–646, doi: 10.1046/J.1365-246X.2000.00109.X.

Aubry, M.-P., Berggren, W.A., Stott, L., and Sinha, A., 1996, The upper Paleocene-lower Eocene stratigraphic record and the Paleocene-Eocene boundary carbon isotope excursion: Implications for geochronology, *in* Knox, R.W.O.'B., et al., eds., Correlation of the early Paleogene in Northwest Europe: Geological Society [London] Special Publication 101, p. 353–380.

Barker, P.F., and Burrell, J., 1977, The opening of Drake Passage: Marine Geology, v. 25, p. 15–34, doi: 10.1016/0025-3227(77)90045-7.

Barker, P.F., Kennett, J.P., O'Connell, S., Berkowitz, S.P., Bryant, W.R., Burckle, L.H., Egeberg, P.K., Fuetterer, D.K., Gersonde, R.E., Golovchenko, X., Hamilton, N., Lawver, L.A., Lazarus, D.B., Lonsdale, M.J., Mohr, B.A., Nagao, T., Pereira, C.P.G., Pudsey, C.J., Robert, C.M., Schandl, E.S., Spiess, V., Stott, L.D., Thomas, E., Thompson, K.F.M., and Wise, S.W., Jr., 1988, Proceedings of the Ocean Drilling Program: College Station, Texas, Initial Reports, v. 113, p. 785.

Barker, P.F., Kennett, J.P., O'Connell, S., Berkowitz, S.P., Bryant, W.R., Burckle, L.H., Egeberg, P.K., Fuetterer, D.K., Gersonde, R.E., Golovchenko, X., Hamilton, N., Lawver, L.A., Lazarus, D.B., Lonsdale, M.J., Mohr, B.A., Nagao, T., Pereira, C.P.G., Pudsey, C.J., Robert, C.M., Schandl, E.S., Spiess, V., Stott, L.D., Thomas, E., Thompson, K.F.M., and Wise, S.W., Jr., 1990, Proceedings of the Ocean Drilling Program: College Station, Texas, Initial Reports, v. 113, p. 1033.

Barrett, P.J., 1996, Antarctic palaeoenvironment through Cenozoic times—A review: Terra Antartica, v. 3, p. 103–119.

Berggren, W.A., Kent, D.V., Flynn, J.J., and van Couvering, J.A., 1985, Cenozoic geochronology: Geological Society of America Bulletin, v. 96, p. 1407–1418.

Berggren, W.A., Kent, D.V., Swisher, C.C., III, and Aubry, M.-P., 1995, A revised Cenozoic geochronology and chronostratigraphy, *in* Berggren, W.A., et al., eds., Geochronology, time scales and global stratigraphic correlation: Framework for an historical geology: SEPM (Society for Sedimentary Geology) Special Publication 54, p. 129–212.

Besse, J., and Courtillot, V., 2002, Apparent and true polar wander and the geometry of the geomagnetic field over the last 200 Myr: Journal of Geophysical Research, v. 107, 2300, doi: 10.129/2000JB000050.

Cande, S.C., and Kent, D.V., 1992, A new geomagnetic polarity time scale for the late Cretaceous and Cenozoic: Journal of Geophysical Research, v. 97, p. 13,917–13,951.

Cande, S.C., and Kent, D.V., 1995, Revised calibration of the geomagnetic polarity time scale for the late Cretaceous and Cenozoic: Journal of Geophysical Research, v. 100, p. 6093–6095, doi: 10.1029/94JB03098.

Cande, S.C., Stock, J.M., Müller, R.D., and Ishihara, T., 2000, Cenozoic motion between east and west Antarctica: Nature, v. 404, p. 145–150, doi: 10.1038/35004501.

Constable, C.G., Tauxe, L., and Parker, R.L., 1998, Analysis of 11 Myr of geomagnetic intensity variation: Journal of Geophysical Research, v. 103, p. 17,735–17,748, doi: 10.1029/98JB01519.

Day, R., Fuller, M., and Schmidt, V.A., 1977, Hysteresis properties of titanomagnetites: Grain-size and compositional dependence: Physics of the Earth and Planetary Interiors, v. 13, p. 260–267, doi: 10.1016/0031-9201(77)90108-X.

DeConto, R.M., and Pollard, D., 2003, Rapid Cenozoic glaciation of Antarctica induced by declining atmospheric CO_2: Nature, v. 421, p. 245–249, doi: 10.1038/NATURE01290.

Diester-Haass, L., and Zahn, R., 1996, Eocene-Oligocene transition in the Southern Ocean: History of water mass circulation and biological productivity: Geology, v. 24, p. 163–166, doi: 10.1130/0091-7613(1996)0242.3.CO;2.

DiVenere, V.J., Kent, D.V., and Dalziel, I.W.D., 1994, Mid-Cretaceous paleomagnetic results from Marie Byrd Land, West Antarctica: A test of post-100 Ma relative motion between East and West Antarctica: Journal of Geophysical Research, v. 99, p. 15,115–15,139, doi: 10.1029/94JB00807.

Ehrmann, W.U., and Mackensen, A., 1992, Sedimentological evidence for the formation of an East Antarctic ice sheet in Eocene/Oligocene time: Palaeogeography, Palaeoclimatology, Palaeoecology, v. 93, p. 85–112, doi: 10.1016/0031-0182(92)90185-8.

Exon, N.F., Kennett, J.P., Malone, M.J., 2001, Proceedings of the Ocean Drilling Program: Initial Reports, v. 189, http://www-odp.tamu.edu/publications/189_IR/189ir.htm (August 2004).

Flower, B.P., 1999, Cenozoic deep-sea temperatures and polar glaciation: The oxygen isotope record, *in* Barrett, P.J., and Orombelli, G., eds., Geological Records of Global and Planetary Changes, Proceedings of the workshop: Terra Antartica Reports, v. 3, p. 27–42.

Fuller, M., Hastedt, M., and Herr, B., 1998, Coring induced magnetization of recovered ODP sediment: Proceedings of the Ocean Drilling Program, Scientific Results, v. 157, p. 47–56.

Glass, B.P., Hall, C.M., and York, D., 1986, $^{40}Ar/^{39}Ar$ laser probe dating of North American tektite fragments from Barbados and the age of the Eocene-Oligocene boundary: Chemical Geology, v. 59, p. 181–186.

Hagelberg, T.K., Pisias, N.G., Shackleton, N.J., Mix, A.C., and Harris, S., 1995, Refinement of a high-resolution, continuous sedimentary section for studying equatorial Pacific Ocean paleoceanography, Leg 138: Proceedings of the Ocean Drilling Program, Scientific Results, v. 138, p. 31–46.

Kennett, J.P., 1977, Cenozoic evolution of Antarctic glaciation, the circum-Antarctic ocean, and their impact on global paleoceanography: Journal of Geophysical Research, v. 82, p. 3843–3860.

Kennett, J.P., 1978, The development of planktonic biogeography in the Southern Ocean during the Cenozoic: Marine Micropaleontology, v. 3, p. 301–345, doi: 10.1016/0377-8398(78)90017-8.

Kennett, J.P., and Barker, P.F., 1990, Latest Cretaceous to Cenozoic climate and oceanographic developments in the Weddell Sea, Antarctica: An ocean drilling perspective: Proceedings of the Ocean Drilling Program, Scientific Results, v. 113, p. 937–960.

Kennett, J.P., Houtz, R.E., Andrews, P.B., Edwards, A.R., Gostin, V.A., Hajos, M., Hampton, M.A., Jenkins, D.G., Margolis, S.V., Ovenshine, A.T., and Perch-Nielsen, K., 1974, Development of the Circum-Antarctic Current: Science, v. 186, p. 144–147.

Kennett, J.P., Houtz, R.E., Andrews, P.B., Edwards, A.R., Gostin, V.A., Hajos, M., Hampton, M., Jenkins, D.G., Margolis, S.V., Ovenshine, A.T., and Perch-Nielsen, K., 1975, Cenozoic paleoceanography in the southwest Pacific Ocean, Antarctic glaciation, and the development of the Circum-Antarctic Current, *in* Kennett, J.P., et al., eds., Initial Reports Deep Sea Drilling Program: Washington, D.C., U.S. Government Printing Office, v. 29, p. 1155–1169.

Kirschvink, J.L., 1980, The least-squares line and plane and the analysis of palaeomagnetic data: Geophysical Journal of the Royal Astronomical Society, v. 62, p. 699–718.

Lawver, L.A., and Gahagan, L.M., 2003, Evolution of Cenozoic seaways in the circum-Antarctic region: Palaeogeography, Palaeoclimatology, Palaeoecology, v. 198, p. 11–37, doi: 10.1016/S0031-0182(03)00392-4.

Lawver, L.A., Gahagan, L.M., and Coffin, M.F., 1992, The development of paleoseaways around Antarctica, *in* Kennett, J.P., and Warnke, D.A., eds., The Antarctic paleoenvironment: A perspective on global change: American Geophysical Union, Antarctic Research Series, v. 56, p. 7–30.

Nagy, E.A., and Valet, J.-P., 1993, New advances for paleomagnetic studies of sediment cores using U-channels: Geophysical Research Letters, v. 20, p. 671–674.

Pearson, P.N., and Palmer, M.R., 2000, Atmospheric carbon dioxide over the past 60 million years: Nature, v. 406, p. 695–699, doi: 10.1038/35021000.

Persico, D., and Villa, G., 2002, High-resolution calcareous nannofossil biostratigraphy and palaeoecology from Eocene-Oligocene sediments, Maud Rise, Weddell Sea, and Kerguelen Plateau, Antarctica: University of Parma, Italy, Abstract 9th International Nannoplankton Association Conference, 8th–14th September 2002.

Persico, D., and Villa, G., 2004, Eocene-Oligocene calcareous nannofossils from Maud Rise and Kerguelen Plateau (Antarctica): Palaeoecological and palaeoceanographic implications: Marine Micropaleontology, v. 52, p. 153–179, doi: 10.1016/j.marmicro.2004.05.002.

Poore, R.Z., Tauxe, L., Percival, S.F., Jr, LaBreque, J.L., Wright, R., Peterson, N.P., Smith, C.C., Tucker, P., and Hsu, K.J., 1983, Late Cretaceous-Cenozoic magnetostratigraphy and biostratigraphy of the South Atlantic Ocean: DSDP Leg 73: Palaeogeography, Palaeoclimatology, Palaeoecology, v. 42, p. 127–149, doi: 10.1016/0031-0182(83)90041-X.

Robert, C., Diester-Haass, L., and Chamley, H., 2002, Late Eocene-Oligocene oceanographic development at southern high latitudes, from terrigenous and biogenic particles: A comparison of Kerguelen Plateau and Maud Rise, ODP Sites 744 and 689: Marine Geology, v. 191, p. 37–54, doi: 10.1016/S0025-3227(02)00508-X.

Roberts, A.P., Cui, Y.L., and Verosub, K.L., 1995, Wasp-waisted hysteresis loops: Mineral magnetic characteristics and discrimination of components in mixed magnetic systems: Journal of Geophysical Research, v. 100, p. 17,909–17,924, doi: 10.1029/95JB00672.

Roberts, A.P., Bicknell, S.J., Byatt, J., Bohaty, S.M., Florindo, F., and Harwood, D.M., 2003, Magnetostratigraphic calibration of Southern Ocean diatom datums from the Eocene-Oligocene of Kerguelen Plateau (Ocean Drilling Program Sites 744 and 748): Palaeogeography, Palaeoclimatology, Palaeoecology, v. 198, p. 145–168, doi: 10.1016/S0031-0182(03)00397-3.

Spiess, V., 1990, Cenozoic magnetostratigraphy of Leg 113 drill sites, Maud Rise, Weddell Sea, Antarctica, *in* Barker, P.F., et al., eds., Proceedings of the Ocean Drilling Program: College Station, Texas, Scientific Results, v. 113, p. 261–318.

Stott, L.D., and Kennett, J.P., 1990, Antarctic Paleogene planktonic foraminifer biostratigraphy: ODP Leg 113, Site 689 and 690: Proceedings of the Ocean Drilling Program, Scientific Results, v. 113, p. 549–569.

Tauxe, L., and Hartl, P., 1997, 11 million years of Oligocene geomagnetic field behaviour: Geophysical Journal International, v. 128, p. 217–229.

Tauxe, L., LaBrecque, J.L., Dodson, R., and Fuller, M., 1983, "U" channels—A new technique for paleomagnetic analysis of hydraulic piston cores: Eos (Transactions, American Geophysical Union), v. 64, p. 219.

Tauxe, L., Mullender, T.A.T., and Pick, T., 1996, Potbellies, wasp-waists, and superparamagnetism in magnetic hysteresis: Journal of Geophysical Research, v. 101, p. 571–583, doi: 10.1029/95JB03041.

Thomas, E., Barrera, E., Hamilton, N., Huber, B.T., Kennett, J.P., O'Connell, S., Pospichal, J.J., Spiess, V., Stott, L.D., Wei, W., and Wise, S.W., Jr, 1990, Upper Cretaceous-Paleogene stratigraphy of Site 689 and 690, Maud Rise (Antarctica), *in* Barker, P.F., et al., eds., Proceedings of the Ocean Drilling Program: College Station, Texas, Scientific Results, v. 113, p. 901–914.

Touchard, Y., Rochette, P., Aubry, M.-P., and Michard, A., 2003, High-resolution magnetostratigraphic and biostratigraphic study of Ethiopian traps-related products in Oligocene sediments from the Indian Ocean: Earth and Planetary Science Letters, v. 206, p. 493–508, doi: 10.1016/S0012-821X(02)01084-1.

Vonhof, H.B., Smit, J., Brinkhuis, H., Montanari, A., and Nederbragt, A.J., 2000, Global cooling accelerated by early late Eocene impacts: Geology, v. 28, p. 687–690, doi: 10.1130/0091-7613(2000)0282.3.CO;2.

Weeks, R., Laj, C., Endignoux, L., Fuller, M., Roberts, A., Manganne, R., Blanchard, E., and Goree, W., 1993, Improvements in long-core measurement techniques: applications in palaeomagnetism and palaeoceanography: Geophysical Journal International, v. 114, p. 651–662.

Wei, W., 1992, Paleogene chronology of Southern Ocean drill holes: An update, *in* Kennett, J.P., and Warnke, D.A., eds., The Antarctic paleoenvironment: A perspective on global change: Antarctic Research Series, v. 56, p. 75–96.

Wei, W., and Thierstein, H.R., 1991, Upper Cretaceous and Cenozoic calcareous nannofossils of the Kerguelen Plateau (southern Indian Ocean) and Prydz Bay (East Antarctica), *in* Barrow, J., et al., eds., Proceedings of the Ocean Drilling Program: College Station, Texas, Scientific Results, v. 119, p. 467–492.

Wei, W., and Wise, S.W., Jr, 1989, Paleogene calcareous nannofossil magnetobiochronology: Results from South Atlantic DSDP Site 516: Marine Micropaleontology, v. 14, p. 119–152, doi: 10.1016/0377-8398(89)90034-0.

Wei, W., and Wise, S.W., Jr, 1992, Eocene-Oligocene calcareous nannofossil magnetobiochronology of the Southern Ocean: Newsletters on Stratigraphy, v. 26, p. 119–132.

Weissel, J.K., and Hayes, D.E., 1972, Magnetic anomalies in the southeast Indian Ocean, *in* Hayes, D.E., ed., Antarctic oceanology (vol. 2): The Australian-New Zealand Sector: American Geophysical Union, Antarctic Research Series, v. 19, p. 165–196.

Witte, W.K., and Kent, D.V., 1988, Revised magnetostratigraphies confirm low sedimentation rates in Arctic Ocean cores: Quaternary Research, v. 29, p. 43–53.

Zachos, J.C., Pagani, M., Sloan, L., Thomas, E., and Billups, K., 2001, Trends, rhythms, and aberrations in global climate 65 Ma to Present: Science, v. 292, p. 686–693, doi: 10.1126/SCIENCE.1059412.

Manuscript Received by the Society 3 December 2003
Revised Manuscript Received 24 May 2004
Manuscript Accepted 29 June 2004

Printed in the USA